Available online at www.sciencedirect.com

ScienceDirect

journal homepage: www.elsevier.com/locate/he

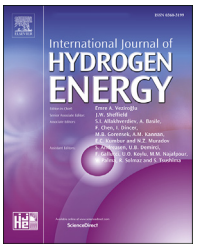

Additive manufacturing for Proton Exchange Membrane (PEM) hydrogen technologies: merits, challenges, and prospects

Ahmad Baroutaji [a,*], *Arun Arjunan* [b,c], *John Robinson* [b,c,d,e], *Mohammad Ali Abdelkareem* [f,g], *Abdul-Ghani Olabi* [h,a]

[a] *School of Engineering and Technology, College of Engineering and Physical Sciences, Aston University, Aston Triangle, Birmingham, B4 7ET, UK*

[b] *Additive Manufacturing of Functional Materials (AMFM) Research Group, Centre for Engineering Innovation and Research, University of Wolverhampton, Telford Campus, Telford, TF2 9NT, UK*

[c] *School of Engineering, Computing and Mathematical Sciences, Faculty of Science and Engineering, University of Wolverhampton, Telford Campus, Telford, TF2 9NT, UK*

[d] *Additive Analytics Ltd., Stirchley Road, Telford, TF3 1EB, UK*

[e] *AceOn Battery Solar Technology Ltd, Unit 9B, Stafford Park 12, Telford, TF3 3BJ, UK*

[f] *Dept. of Sustainable and Renewable Energy Engineering, University of Sharjah, P.O. Box 27272, Sharjah, United Arab Emirates*

[g] *Chemical Engineering Department, Minia University, Elminia, Egypt*

[h] *Sustainable Energy and Power Systems Research Centre, University of Sharjah, P.O.Box: 27272, Sharjah, United Arab Emirates*

HIGHLIGHTS

- The AM technologies relevant to PEM fabrication are reviewed.
- Corrosion performance of AM materials in the PEM working environment is presented.
- The challenges and prospects of AM for PEM fabrication are discussed.
- AM has the potential to revolutionize the fabrication of PEM systems.

ARTICLE INFO

Article history:
Received 21 February 2023
Received in revised form
18 May 2023
Accepted 5 July 2023
Available online xxx

Keywords:
Additive manufacturing
3D printing
Fuel cell
Electrolyser

ABSTRACT

With the growing demand for green technologies, hydrogen energy devices, such as Proton Exchange Membrane (PEM) fuel cells and water electrolysers, have received accelerated developments. However, the materials and manufacturing cost of these technologies are still relatively expensive which impedes their widespread commercialization. Additive Manufacturing (AM), commonly termed 3D Printing (3DP), with its advanced capabilities, could be a potential pathway to solve the fabrication challenges of PEM parts. Herein, in this paper, the research studies on the novel AM fabrication methods of PEM components are thoroughly reviewed and analysed. The key performance properties, such as corrosion and hydrogen embrittlement resistance, of the additively manufactured materials in the PEM working environment are discussed to emphasise their reliability for the PEM systems. Additionally, the major challenges and required future developments of AM technologies to unlock their full potential for PEM fabrication are identified. This paper provides insights

* *Corresponding author.*
E-mail address: a.baroutaji@aston.ac.uk (A. Baroutaji).

https://doi.org/10.1016/j.ijhydene.2023.07.033

SLM
IJP

from the latest research developments on the significance of advanced manufacturing technologies in developing sustainable energy systems to address the global energy challenges and climate change effects.

Introduction

The damaging effects of climate change and global warming continue to pose real threats to our environment. Bushfires, droughts, ice sheet melting, floods, and depletion of food and water are among the unfavourable consequences of global warming on our planet and society. Reducing the reliance on fossil fuels and adopting more clean and Renewable Energy Sources (RESs) are the only avenues to beat global warming [1]. Hydrogen is always debated as the low-carbon energy carrier of the future because it only emits water and heat as by-products of the energy production process. Among the different hydrogen fuel cell technologies, Proton Exchange Membrane Fuel Cell (PEMFC) carries significant potential to be a key player in the transition to the hydrogen economy. PEMFC is featured by low operational temperature, zero noise, fast start-up, high energy density, high electrical efficiency, and long operational lifespan which gives this technology significant advantages over its competitors [2,3]. PEMFC has been widely considered as an energy conversion technology for various sectors such as maritime [4,5], automotive [6], aerospace [7], energy storage [8], portable devices [9], and sustainable buildings [10,11].

In addition to the fuel cells, the transition to the hydrogen economy requires developing more sustainable hydrogen production techniques. Hydrogen can be produced from different feedstocks such as hydrocarbons, biomass, and water through different electrochemical, thermochemical, and biochemical processes such as steam reforming, pyrolysis, electrolysis, and gasification [12–14]. Electrolysis of water is considered the most capable route to generate clean hydrogen because the process does not yield carbon emissions and only produces oxygen as a by-product. In fact, producing hydrogen using RESs-powered electrolysers and then using it in fuel cells to generate electricity is one of the most promising sustainable energy solutions. Among the different water electrolysis technologies, Proton Exchange Membrane Water Electrolyser (PEMWE) stands out due to its high production rate of pure hydrogen and high energy efficiency [15].

Despite the promising potential of the PEM technologies, their share in the energy market is still relatively low due to some barriers such as high product cost, low reliability, and high maintenance and repairs costs [16]. These barriers reduce end-user acceptance and impede the commercialization of the technology. In the past three decades, significant industrial and academic research efforts were placed to tackle the PEM challenges and develop reliable low-cost technology. Most of the academic work focused on design development aspects where various experimental, modelling, and optimization tools were used to find the optimal design and operating parameters of such technologies [17–19]. On the other side, only limited research attention has been paid to the fabrication and production processes of the PEM components. In fact, the manufacturing challenges are regarded as the main barriers hindering the large-scale commercialization of PEM technologies [20]. Adopting novel manufacturing technologies, such as AM (3DP), may assist in addressing the manufacturing challenges of PEM technologies. AM refers to different digital manufacturing techniques that can produce a part layer-by-layer directly from a computer-aided design (CAD) model without the need for any part-specific tools [21]. AM has provided distinct advantages over Conventional Manufacturing (CM) methods in terms of higher design freedom, higher precision levels, more automated production, fewer fabrication steps, and fewer post-manufacturing needs leading to material and energy savings, shorter product development cycle, more flexible and efficient product design, and less negative influences on the environment [22–25]. Besides the above, AM can be used for on-demand product manufacturing closer to the consumption sites resulting in reduced demand for long transport journeys and the associated possible environmental pollution [24]. AM technologies are receiving increased adoption in different industries such as aerospace [26], automotive [27], biomedical [28–30], construction [31], fashion and jewellery [32], and energy [33–36]. In the energy sector, AM is used for fabricating key components such as energy materials [37], heat exchangers [30,38], batteries [39], components with functional fluidic channels [40], catalytic technologies [41], electrically conductive polymers [42], chemical reactors [43], etc.

AM (3DP), with its huge potential, laid itself among the possible solutions to revolutionize the fabrication of PEM systems [44]. A noticeable amount of research articles has been published recently on using different AM technologies for PEM fabrication. The use of AM for producing PEM parts is a step in the right direction and may improve the Manufacturing Readiness Level (MRL) of PEM technologies which is lower than the comparable technologies [45]. Thus, to evaluate the potential of AM methods as effective fabrication pathways for PEM technologies, it is important to systemically analyse their benefits and limitations from both technical and economic perspectives. Therefore, this paper aims to present a comprehensive overview of the recent developments in the use of AM methods for manufacturing the next generation of PEM systems focusing on their merits, challenges, and possible solutions to take them forward. As the materials used in the PEM should withstand its harsh working environment,

Please cite this article as: Baroutaji A et al., Additive manufacturing for Proton Exchange Membrane (PEM) hydrogen technologies: merits, challenges, and prospects, International Journal of Hydrogen Energy, https://doi.org/10.1016/j.ijhydene.2023.07.033

the performance of the additively manufactured components in the PEM working environment is emphasized and discussed in this review to ensure their reliability for PEM applications. The paper is structured as follows; first, an overview of PEM components and working principles is given. Second, the different AM techniques that have been used for PEM applications are introduced and explained. Third, the research studies concerned with the fabrication and performance of Additively Manufactured (AMed) fuel cell components are reviewed. Forth, the investigations focused on the corrosion and hydrogen embrittlement responses of AMed materials in PEM working environments are presented. Fifth, the advantages, challenges, and future research directions of AM for PEM devices are discussed.

Overview of PEMFC and PEMWE

PEMFC and PEMWE are the two main PEM hydrogen technologies. PEMFC is an energy conversion technology for producing electricity from the chemical reaction between hydrogen and the air; and generates water as a by-product. The PEMFC can be either Low Temperature (LT-PEMFC) operating at 60–80 °C or High Temperature (HT-PEMFC) operating at 120–200 °C. On the other side, PEMWE is an electrochemical device that produces hydrogen from water using electrical energy; and generates oxygen as a by-product [15].

PEM technologies use a solid polymer membrane as an ion-conducting electrolyte which is sandwiched between the anode and the cathode. The main components of each of the anode and the cathode are Catalyst Layer (CL) or electrode, Gas Diffusion Layer (GDL), and Bipolar Plate (BPP). The membrane and CL are commercially fabricated as one part known as Membrane Electrode Assembly (MEA). In addition to the main components, PEM devices contain secondary parts such as Current Distributor (CD), sealants, Cooling Plates (CPs), and end plates. The working principles of PEMFC and PEMWE are schematically explained in Fig. 1 while the requirements and common materials of their main components are summarized in Table 1.

MEA is the heart of the PEM system responsible to deliver the hydrogen cations (H^+) from the anode to the cathode. The commercial MEAs can be either three-layer or five-layer. The three-layer MEA, also called Catalyst Coated Membrane (CCM), consists of the membrane and two CLs. Similarly, the five-layer MEA composes of the membrane, two CLs, and two GDLs. The commonly used membrane in PEM devices is perfluorosulfonic acid polymer (PFSA), commercially traded under the name Nafion [46]. Nafion is a high-cost material, and its ion conductivity drops at high temperatures therefore it is not suitable for HT-PEMFC [47]. HT-PEMFC uses Polybenzimidazole (PBI) membrane because it is less water dependent and can maintain high ionic conductivity at high temperatures [47]. PEM devices use carbon-supported platinum (Pt/C) as a catalyst which is deposited on either the membrane forming CCM or the GDL forming Gas Diffusion Electrode (GDE). The platinum-based catalysts are expensive and form around 35% of the whole PEM stack cost [48,49]. The current MEA production route is a non-continuous and cumbersome process with multiple and independent steps. The three-layer MEA, i.e. CCM, is produced by fabricating the membrane and then adding the catalyst on it using different ink deposition methods, such as slot-die coating, knife coating, spray painting, screen printing, and Inkjet Printing (IJP) [50,51]. The five-layer MEA is produced by preparing the GDLs and CCM separately which are then assembled by tempered lamination or ultrasonic bonding [51,52].

GDL, may also be referred to as Porous Transport Layer (PTL), is a fibrous porous medium sandwiched between the CL and the BPP; and it is responsible for transferring the electrons, reactants, and heat between them. GDLs form pathways for the reactive gases from the BPP to the MEA ensuring a uniform distribution of these gases over the surfaces of the electrodes [53]. The main requirements of the GDL are (i) water permeability to allow water transport from/to the catalyst layer, (ii) reactants permeability to facilitate the supply of hydrogen and oxygen to the active sites on the MEA, (iii) electronic conductivity to transfer the electrons from the active sites, (iv) thermal conductivity to provide effective heat transport and uniform heat distribution, and (v) adequate mechanical strength and high corrosion resistance. The performance of the PEM devices is highly influenced by the structural and mass transport characteristics of the GDLs. Highly electron conductive carbon papers, which are manufactured via high temperature carbonization of a thermosetting resin, are typically considered as suitable GDL for PEM devices [54]. Metallic materials have also received increased attention for fabricating GDLs due to their high thermal and electric conductivity, low cost, and fast production [55,56].

BPP is another key component of PEMFC and PEMWE and play an important role in both the performance and durability of the system [57]. For effective operation of the PEM system, BPPs must satisfy various technical features including good thermal and electrical conductivities, high corrosion resistance in the presence of oxygen, high resistance to hydrogen embrittlement, and good mechanical strength [58]. The BPPs feature a complex network of flow channels responsible for delivering the hydrogen and oxygen gases to the GDLs [59]. Also, BPPs contribute to the removal of reaction by-products including water and heat [60]. The performance of a PEM device depends hugely on the flow field configuration of the BPP. The flow field with good design should provide uniform distribution of the reactants, minimum pressure drops, and effective thermal and water management [61]. Therefore, the geometrical configuration of the BPP has received a good deal of research resulting in different flow-field designs such as parallel, serpentine, pin, and interdigitated structures [62]. The BPPs are mainly made of graphite-based or metallic-based materials [63]. The poor mechanical properties of graphite-based BPP formed a serious concern for the durability of the PEM systems [64,65]. In this regard, metallic-based BPPs provide an excellent combination of good mechanical strength, and high electrical and thermal conductivities allowing them to have significant competitive advantages over other materials. However, the metallic BPPs have comparatively lower corrosion resistance than the graphite ones and therefore they tend to have a shorter service life. Metallic BPPs are normally coated with an anti-corrosive layer to enhance their corrosion performance. The materials and manufacturing bill of BPPs forms around 30%–40% of the total PEM device cost [66,67]. According to the International Renewable Energy

Please cite this article as: Baroutaji A et al., Additive manufacturing for Proton Exchange Membrane (PEM) hydrogen technologies: merits, challenges, and prospects, International Journal of Hydrogen Energy, https://doi.org/10.1016/j.ijhydene.2023.07.033

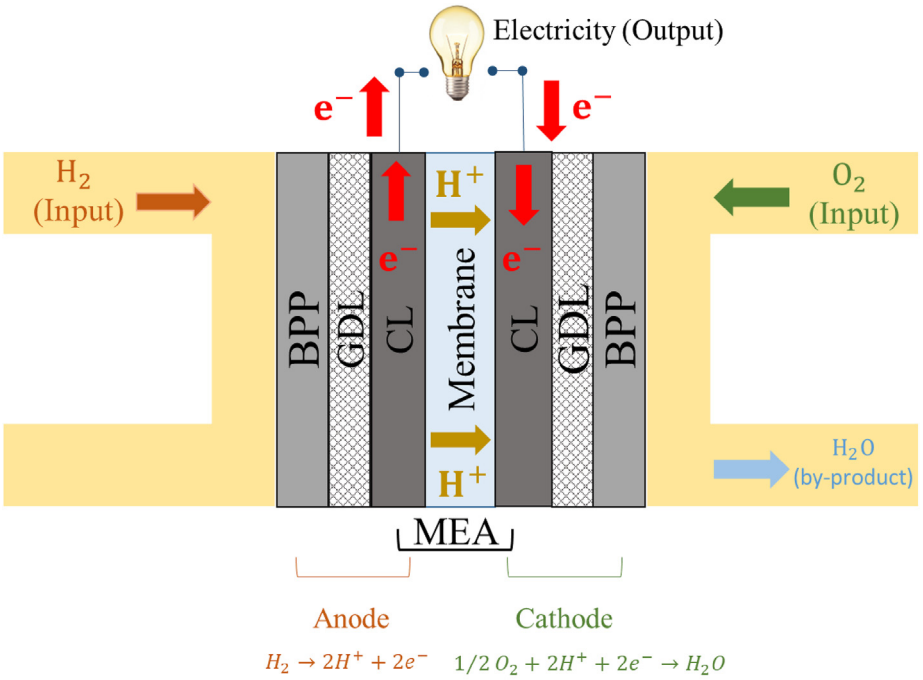

(a)

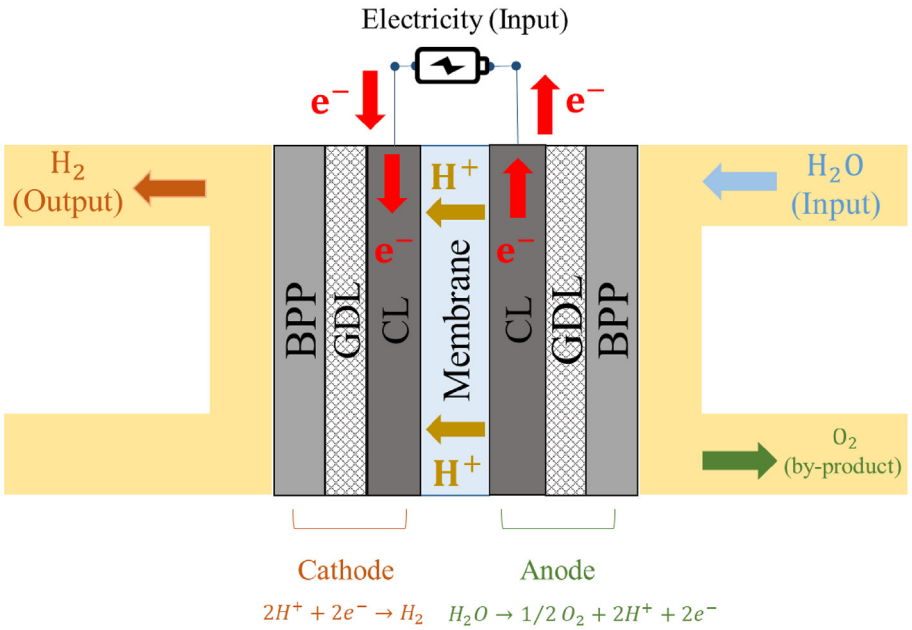

(b)

Fig. 1 – Main components and working principles of (a) PEMFC (b) PEMW.

Agency (IRENA) report, BPP is a significant cost part within PEMWE as its cost can reach up to 23.9% of the overall cost of the device [68]. The graphite-based BPPs are created by a moulding process, such as injection moulding and compression moulding, while the metallic-based BPPs can be obtained by hydroforming, electromagnetic forming, hollow embossing

Please cite this article as: Baroutaji A et al., Additive manufacturing for Proton Exchange Membrane (PEM) hydrogen technologies: merits, challenges, and prospects, International Journal of Hydrogen Energy, https://doi.org/10.1016/j.ijhydene.2023.07.033

Table 1 – Function, requirements, and materials of the main components of PEM devices.

Component	Main function	Requirements	Common materials
BPP	Deliver the reactants to the anode and the cathode	High thermal conductivity High electrical conductivity High corrosion resistance High resistance to hydrogen embrittlement Good mechanical strength	• Graphite • Metals (Stainless steel, Aluminium, Titanium)
GDL	Disperse the reactants from BPP over the CL	Good water and reactants permeability High electronic conductivity High thermal conductivity Good mechanical strength High corrosion resistance	• Carbon paper • Metallic micro-channel mesh
CL	Trigger and increase the rate of the anodic and the cathodic reactions	High specific surface area	Carbon-supported platinum (Pt/C)
Membrane	Transfer the hydrogen cations from the anode to the cathode	High ionic conductivity within a wide range of temperatures Impermeable to gases Durable Hight chemical stability Resistant to chemical attack	• Nafion (LT-PEMFC and PEMWE) • PBI (HT-PEMFC)

rolling, stamping, milling (CNC machining), micro-electrochemical machining, laser ablation, etc. [58,69–71]. Despite that such fabrication technologies were proved to be efficient for mass production, they normally cause significant materials waste and are not suitable to produce very complex and customized geometries, particularly those with large cavities and internal channels [72,73].

Overview of AM fabrication methods

AM can be defined as a computer-controlled fabrication process for creating parts by depositing materials layer by layer. The AM process starts with creating an initial 3D CAD model of the part. Then, a 3DP slicer software is used to prepare the CAD model for AM by slicing it into successive layers and generating a G-Code (set of instructions) to control the AM system [74]. The G-Cod is then transferred to the AM system to start the layer-by-layer building process. Following the building process, the part is extracted from the AM system where the extra support structures are removed and any necessary post-building processes, such as cleaning, polishing, and heat treatment, are completed before obtaining the final product. The typical steps of creating a part using AM are shown in Fig. 2.

According to ISO/ASTM 52900:2015 standard, there are seven main categories of AM including Photopolymerization (VP), Material Jetting (MJ), Binder Jetting (BJ), Material Extrusion (ME), Directed Energy Deposition (DED), Sheet Lamination (SL), and Powder Bed Fusion (PBF) [75,76]. The AM techniques relevant to PEM fabrication are Selective Laser Melting (SLM), Selective Laser Sintering (SLS), and Electron Beam Melting (EBM) which are PBF techniques, Inkjet Printing (IJP) which is MJ technique, and Fused Deposition Modelling (FDM) which is ME technique. Fig. 3 summarizes the main AM technologies and the subcategories used for PEM devices. In this section, the AM techniques that have been used for PEM fabrication are discussed.

PBF techniques

The PBF techniques use fine powder as raw material, i.e. feedstock, and a heat source, either Laser Beam (LB) or Electron Beam (EB), to induce melting or sintering in the powder particles [77–79]. The building process starts with depositing a layer of the material powder on the building platform and subsequently using the thermal energy source to fuse the powder in certain locations of the powder bed corresponding to the geometry of the part. The process of spreading and fusion the powder is repeated until creating the final part. An inert environment is normally created within the building space to minimize oxidation during the process. The PBF can be divided into SLM, also known as Laser Powder Bed Fusion (L-PBF), EBM, and SLS, also known as Direct Metal Laser Sintering (DMLS) when it is used for metallic materials. High power-density focused laser (photon) and electron beams are used to melt the material in SLM and EBM, respectively. In SLS, the LB does not melt the powder particles but just heats them to the sintering level so they can fuse together [80]. PBF can be used with a variety of materials including metals, ceramics, polymers, and composites. Within the field of PEM fabrication, SLM is the most used PBF technique for manufacturing metallic parts and therefore some further details about this process are provided in the remaining of this section.

The quality of the SLM parts depends on a wide range of material and process parameters that should be precisely controlled to achieve a successful print. The material parameters include material composition and powder characteristics, i.e., shape and size of powder particles, while the process parameters include laser power (P), scan speed (v), hatch distance (h), layer thickness (t), and scanning strategy. The process parameters affect the energy density (E) supplied at the powder bed which can be calculated using Eq. (1).

$$E = \frac{P}{v \times h \times t} \quad \text{Eq. 1}$$

Please cite this article as: Baroutaji A et al., Additive manufacturing for Proton Exchange Membrane (PEM) hydrogen technologies: merits, challenges, and prospects, International Journal of Hydrogen Energy, https://doi.org/10.1016/j.ijhydene.2023.07.033

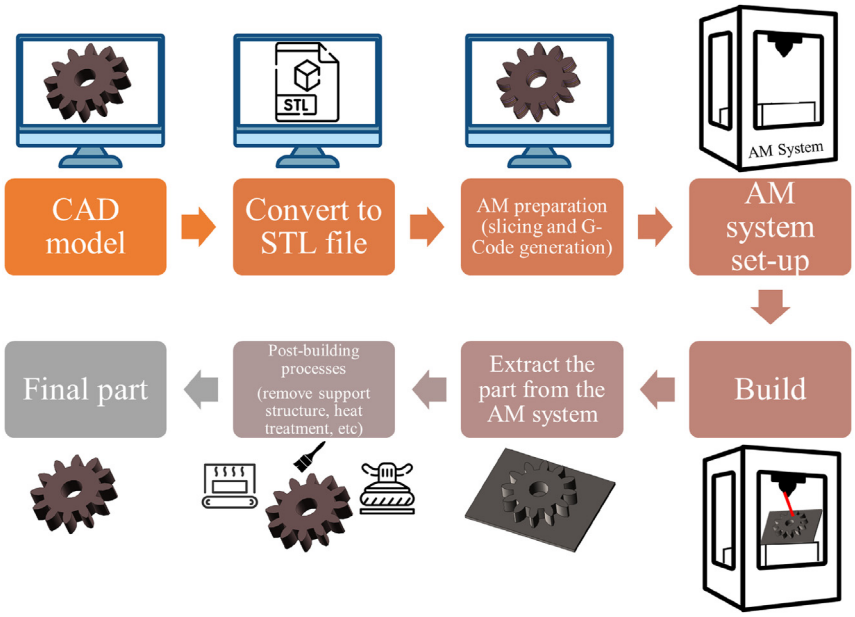

Fig. 2 – Typical steps for creating a part using AM.

The fast heating and solidification cycle associated with SLM processes is the source of different defects that affects the structural integrity and the quality of the printed part impeding the adoption of the Selectively Laser Melted (SLMed) parts in some industries [26]. During SLM, the material is subjected to extremely high local temperatures (up to 2500 °C), high cooling rates (10^5–10^7 K/s), and heating, or re-melting, of the underlying materials. Due to such conditions, the metal molecules are arranged in a higher energy state within the SLMed part which in turn shows; a heterogeneous microstructure containing internal stresses, inclusions, and non-equilibrium phases; as well as various metallurgical imperfections such as porosities, micro-cracks, dislocated cells, un-melted powder, and rough surfaces. Post-SLM polishing and heat treatment are normally used to alleviate the influences of these defects and to enhance the mechanical properties of the SLMed parts.

DED

In this method, both the raw material and the thermal energy are supplied simultaneously during the printing process. A heat source, typically LB, EB, or electrical arc, is used to melt the material as it is deposited. DED is normally employed for metallic materials where the feedstock can be either powder or wire. The wire has higher material efficiency but lower resolution while the powder has greater deposition accuracy [26]. The material is supplied from a nozzle which is mounted on a robotic multi-axis movable arm allowing to deposit the material from different angles and directions. DED is

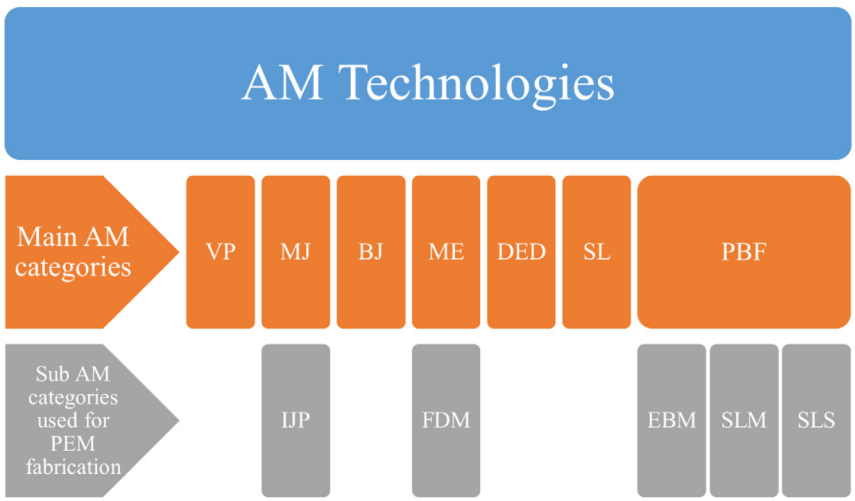

Fig. 3 – Main AM techniques and the subcategories used for PEM fabrication.

Please cite this article as: Baroutaji A et al., Additive manufacturing for Proton Exchange Membrane (PEM) hydrogen technologies: merits, challenges, and prospects, International Journal of Hydrogen Energy, https://doi.org/10.1016/j.ijhydene.2023.07.033

commonly used to repair a valuable existing part, such as a turbine blade, but it can also be used to create new components [81]. It is particularly useful for manufacturing large-size parts as it has less restrictions in terms of dimensions because it does not use a powder bed [26]. DED is faster and cheaper but more complex than PBF. Compared to PBF, DED uses higher energy density and has lower cooling rate, around 10^3–10^5 K/s, resulting in higher porosity levels and coarser microstructure [82]. DED is referred to it using other terminologies including Direct Metal Tooling (DMT), Direct Metal Deposition (DMD), and Laser Engineered Net Shaping (LENS).

IJP

IJP is a non-contact droplet-based direct material deposition technology [83]. It has multi-material deposition capability allowing for creating complex patterns with high resolution [21]. IJP machine, i.e., printer, utilizes a nozzle head to eject material, i.e., ink, onto the substrate without direct contact between the substrate and the printer head. The printer head is normally mounted at around 1 mm above the substrate and the ink flows out of the nozzle at a velocity of 5–10 m/s [84]. A pressure chamber, located behind the printing nozzle, is used to propagate a pressure pulse responsible for forming the liquid drops. The drops, ejected from the nozzle, hit the substrate surface where their post-impact behaviour is driven by inertial, capillary, and gravitational forces.

Ink-like liquid materials are normally used in IJP. Such materials are formed by dispersing active materials in a solvent. The ink should be well formulated with no conglomerates to allow material deposition without clogging the printer nozzle. The ink's physical properties such as viscosity (μ), density (ρ), and surface tension (σ) along with the diameter of the nozzle (d) play an important role in the stability of the formed drops. The stability of the inkjet drop is normally assessed using a parameter Z which can be obtained according to Eq. (2).

$$Z = \frac{\sqrt{\rho d \sigma}}{\mu} \quad \text{Eq. 2}$$

If the Z value of ink is in the range of 1–10, then the ink is expected to form stable droplets.

FDM

FDM, also referred to as Fused Filament Fabrication (FFF), is a cost-effective, simple, and common extrusion-based AM method mainly used for fabricating plastic materials [85]. The feedstock in FDM is filament made from different materials such as Polylactic Acid (PLA), Acrylonitrile Butadiene Styrene (ABS), polyvinyl alcohol (PVA), polycarbonate (PC), and carbon fibre. The building process in FDM involves heating the filament, in the extruder, to the melting point and then depositing it through the extruder head on a building base. The material continues to flow out the extruder head building the part layer-by-layer. The extruder is a computer-controlled moving heated nozzle. The building base is normally made of thick material, such as glass, and can be either hot or cold. The hot building base should be used for materials with a high thermal expansion coefficient as the cold base may cause poor adhesion or induces shrinkage in the deposited material leading to warping in the fabricated component.

Additively manufactured PEM parts

This section presents and discusses the literature studies on AMed components of PEMFC and PEMWE including GDL, BPP, MEA, and other relevant parts.

GDL

Mo et al. [86] used EBM to fabricate titanium mesh as GDL with excellent corrosion resistance and high electric and thermal conductivities for application in PEMWE. The performance of the GDL was characterized in-situ using Modular Galvano (MG) and Galvano Electrochemical Impedance Spectroscopy (GEIS); and ex-situ via Scanning electron microscopy (SEM) and X-ray diffraction (XRD). The 3D printed GDL was compared to the conventional woven and sintered one showing 8% electrolysis performance enhancement due to significant reductions of ohmic losses. The authors reported that EBM is a fast and cheap fabrication method that can produce GDL with highly complex 3D shapes and customized pore morphology. Agudelo et al. [87] created GDL, for the anode side of HT-PEMFC, made of Stainless Steel (SS) 316 L via SLM process. The SLMed GDL has a tubular shape with porosity of 14%–16%, as shown in Fig. 4. The performance of the fuel cell with the SLMed GDL was assessed using electrochemical characterization and a short-term stability test. The GDL with 16% porosity showed the best performance yielding peak power density of 329.25 W/m^2 and a voltage of 0.61 V at 0.1 A. The study confirmed the suitability of SLM techniques for developing innovative GDL for the next generation of PEMFCs. Jayakumar et al. [88] 3D-printed Alumide (aluminum-polyamide composite) substrate using SLS for GDL applications in PEMFC. After printing, graphene-based material was used to coat the substrate generating the final GDL. The synthesized GDL was characterized for its surface morphology, electrical conductivity, and mechanical strength. It was reported that the Selectively Laser Sintered (SLSed) GDL had good mechanical and electrical properties and can be considered as a promising GDL for future PEMFC technology. In particular, it was found that the thickness of the SLSed GDL is less than the standard one implying a less ohmic resistance and higher power density of the device.

BPP

The early work of using AM for BPPs involved manufacturing the BPPs from graphite or plastic materials and then applying an electrically conductive coating layer on their surfaces. Chen et al. [89] fabricated graphite-based BPP for PEMFC via SLS. A powder mixture of graphite and phenolic was used to build the parts. Post-building processes, including carbonization and liquid epoxy infiltration, were applied to the printed part to densify it and reduce its gas permeability. The SLSed BPP exhibited promising performance in terms of good surface finish and mechanical strength. However, the geometrical dimensions of the printed BPP were not very accurate due to

Please cite this article as: Baroutaji A et al., Additive manufacturing for Proton Exchange Membrane (PEM) hydrogen technologies: merits, challenges, and prospects, International Journal of Hydrogen Energy, https://doi.org/10.1016/j.ijhydene.2023.07.033

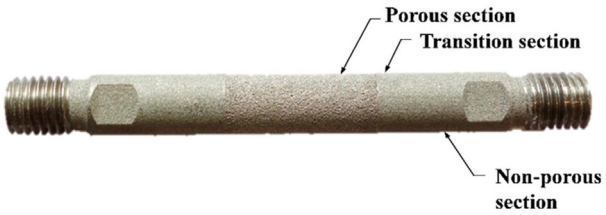

Fig. 4 – Tubular GDL for the anode side of HT-PEMFC fabricated via SLM [87].

dimensional shrinkage that took place during the post-building processes. Compared to the traditional machining of graphite BPP, the SLS was reported to be useful for reducing material and costs. Bourell et al. [90] expanded the previous work by evaluating the influence of carbon fibre additions on the strength and electrical conductivity of the SLSed graphite-based BPP. Chopped carbon fibre was added to the powder mixture of graphite and phenolic. It was found that carbon fibre additions increased the strength but lowered the conductivity of the BPP. Hudkins et al. [91] suggested a rapid prototyping methodology involving metal coating and AM to fabricate BPP for PEMWE. The plates, with serpentine flow-field, were 3D-printed from conductive PLA and then coated with a layer of nickel using an electrodeposition technique. The electrochemical performance of the 3D-printed electroplated PLA plate was found to be superior to that of both nickel and uncoated 3D-printed PLA plates. Chisholm et al. [92] investigated the electrochemical performance of silver-coated 3D-printed anode BPP of PEMWE. FDM was used to build the plates layer-by-layer from polypropylene and then electrodeposition was used to add silver coating on their surfaces, as shown in Fig. 5. Electrochemical Impedance Spectroscopy (EIS), polarization, and durability tests were conducted to explore the performance of the PEMWE. The electrolyser, with the 3D-printed BPP, showed excellent performance measures in terms of current-voltage response, efficiency, and internal resistances. The measured energy and Faradaic efficiencies of the electrolyser are 70% and 94%, respectively.

AM of plastic BPPs proved to be infeasible as such BPPs require adding a coating layer on their surface to make them electrically conductive. Therefore, researchers investigated the additive manufacturing of BPPs made entirely from metals with good electrical and mechanical properties without the need for a plastic core. In this regard, Dawson et al. [93] explored SLM as a potential fabrication method for metallic BPPs made of SS 316 L for application in PEMFC. The performance of the SLMed plate was assessed experimentally and compared to the normal machined one. The contact resistance and polarization responses of SLMed plates were found to be slightly better than the conventionally manufactured ones. Yang et al. [94] additively manufactured SS 316 L BPP using SLM for PEMWE, as shown in Fig. 6. The 3D-printed plate featured a parallel flow-field that acted as a cathode bipolar plate and a current distributor. It was reported that the SLMed BPP has similar elemental weight percentages (wt%) to the raw powder as well as uniform elemental distribution with very limited oxidization. The PEMWE cell with the SLMed BPP exhibited excellent performance producing hydrogen at 1.779 V and 2.0 A/cm^2 and yielding an efficiency of 83.4%. Lyons and Gould [95] used DMLS to manufacture titanium BPPs. The 3D-printed plates featured serpentine and parallel flow-fields for air and fuel, respectively, along with internal channels for coolant flow, as shown in Fig. 7. The plates were coated with a layer of Au/TiO_2 using a thermal spray process to enhance the corrosion resistance and electrical conductivity. Also, the plates were polished to reduce their surface roughness to 1.6 μm and to improve their surface contact with the GDL reducing the overall interfacial resistance within the cell. Upon the assembling of the stack components, it was observed that the 3D-printed BPPs were slightly warped causing a reduction in the stack performance due to leaking and poor electrical contact. Huang et al. [72] adopted SLM to manufacture SS 316 L BPPs with two flow-field configurations including square mesh and obstruction mesh, as shown in Fig. 8. The particle size of the SS powder was in the range of 20 μm–53 μm to ensure complete melting during the SLM fabrication assisting in reducing the surface roughness of the flow channel. The fabricated BPPs were used as the cathode

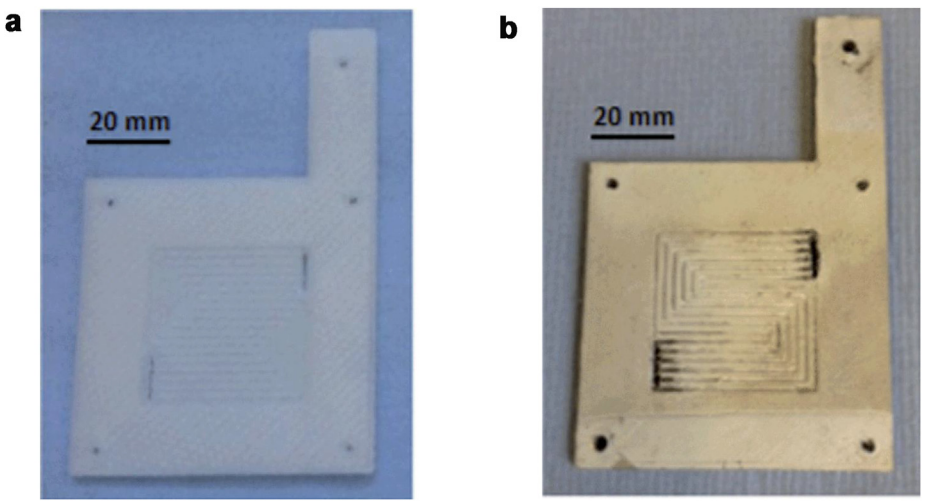

Fig. 5 – 3D-printed polypropylene BPP for PEMWE: (a) bare BPP (b) silver-coated BPP [92].

Please cite this article as: Baroutaji A et al., Additive manufacturing for Proton Exchange Membrane (PEM) hydrogen technologies: merits, challenges, and prospects, International Journal of Hydrogen Energy, https://doi.org/10.1016/j.ijhydene.2023.07.033

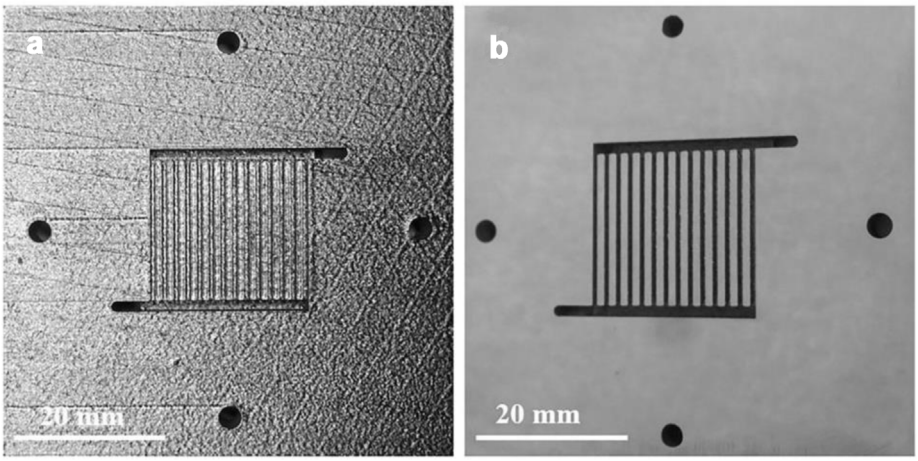

Fig. 6 – SLM-fabricated stainless steel BPP (a) before polishing (b) after polishing [94].

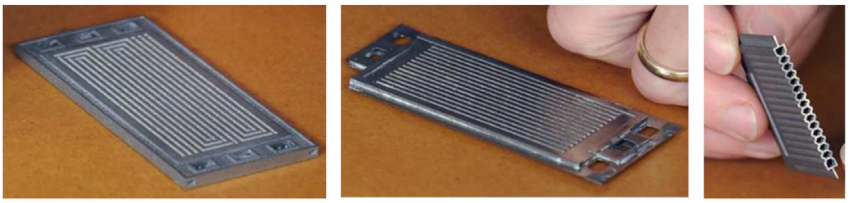

Fig. 7 – DMLS-manufactured titanium BPPs [95].

and assembled into a single PEMFC where the polarization tests were conducted. It was found that the sizes of the SLMed structures are slightly different from the designed ones due to spheridization and curling of square and obstruction edges during the SLM process. It was advised that such effects can be reduced by decreasing the scanning speed and optimizing the scanning path. On the other side, average surface roughness in the range of 0.48 μm–0.52 μm was recorded for the SLMed BPP that was deemed to be acceptable for such applications. It was reported that the SLMed BPP can contribute to enhancing the volumetric specific power of PEMFC devices as it had a thickness of 1 mm that is 80% less than the traditional graphite plate. Zhang et al. [96] fabricated 316 L stainless steel bipolar plates with different flow field designs using SLM. Surface treatment operations, including polishing and sand-blasting, were used to improve the surface quality of SLMed BPPs. It was reported that the SLM process can produce BPP with excellent forming quality, low forming error of less than 4%, and low surface roughness of 0135 μm. Scotti et al. [73] used 3DP to produce BPP for micro PEMFC. SS 316 L powder was used to additively manufacture, using SLM, three different versions of BPPs with square pillar flow-fields, as shown in Fig. 9. It was reported that the SS 316 L powders with a smaller particles' size are beneficial to provide better dimensional control for the SLMed plates. Overall, the micro PEMFCs with the SLMed BPPs exhibited excellent performance with maximum current and power densities of 1.2 A cm^{-2} and 238 W cm^{-2}, respectively. Scotti et al. [97] expanded the

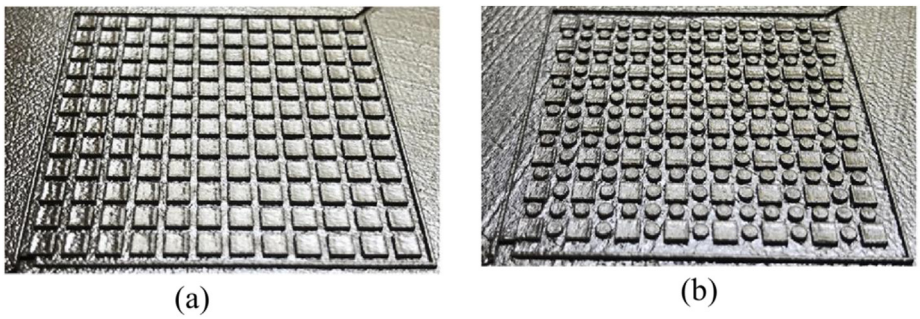

Fig. 8 – SLM-manufactured stainless steel BPPs: (a) square mesh (b) obstruction mesh flow fields [72].

Please cite this article as: Baroutaji A et al., Additive manufacturing for Proton Exchange Membrane (PEM) hydrogen technologies: merits, challenges, and prospects, International Journal of Hydrogen Energy, https://doi.org/10.1016/j.ijhydene.2023.07.033

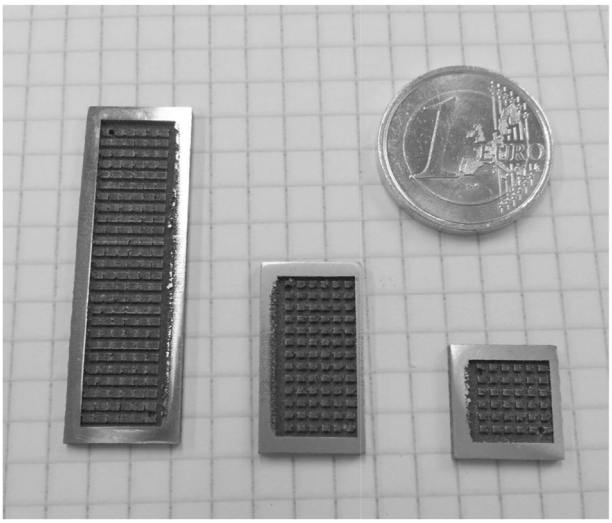

Fig. 9 – 3D-printed stainless steel BPPs for micro PEMFC [73].

previous work by investigating different BPPs with enclosed and open flow-fields, as shown in Fig. 10, for micro PEMFCs. The plates were printed from SS 316 L powders using SLM. The PEMFC with enclosed flow-field plates outperformed that with open flow-field. This performance enhancement was rationalised by the lower Area Specific Resistance (ASR) and the higher contact area between the BPP and GDL provided by such design. It was reported that the micro PEMFC with SLMed stainless steel BPPs were more robust and showed better performance than those cells made from silicon and polymers investigated previously. Sánchez-Molina et al. [66] compared the additively manufactured and conventionally machined plates made of SS 316 L for BBPs application in PEMWE. The plates were made with a parallel flow-field, as shown in Fig. 11 (a), while SLM was used as the AM fabrication method. The performance of the samples was assessed using in-situ polarization curves. The authors observed that the surface roughness of the plates made by AM is noticeably big and indicated that these plates should be polished to obtain comparable surface roughness to that of the machined plates. Additionally, the in-situ polarization curves from both materials, shown in Fig. 11 (b), were very comparable. It was concluded that SLM is a viable method for manufacturing metal BPPs with complex flow distribution channels and appropriate properties to fulfil their role. Trogadas et al. [98] adopted SLS to produce novel SS BPP with lung-inspired fractal flow-fields with a different number of branching generations (N), as shown in Fig. 12. The bio-inspired design with four branching generations outperformed the conventional design with a serpentine flow-field because it produced a more uniform distribution of the reactants over the catalyst layer.

Coating layers can also be used with the AMed metallic BPPs to enhance their properties, mainly increasing the Corrosion Resistance (CR) and reducing the Interfacial Contact Resistance (ICR), leading to improved performance of the PEM system. Yang et al. [99] used a protective coating of thin film gold (Au) on the SLMed SS 316 L BPP for both the anode and cathode of PEMWE. It was found that the coated 3D-printed SS BPP exhibit lower ICR and higher in-situ efficiency than the bare 3D-printed SS and graphite BPPs as can be seen in Fig. 13. This was attributed to the high electrical conductivity of the coating layer which helps in reducing the ohmic resistance within the PEMWE. Gould et al. [100] 3D-printed BPPs using SLS and titanium alloy; and then coated them with a layer of titanium dioxide and gold microdots (Au/TiO_2). The manufactured plates were tested in both a single PEMFC cell and a

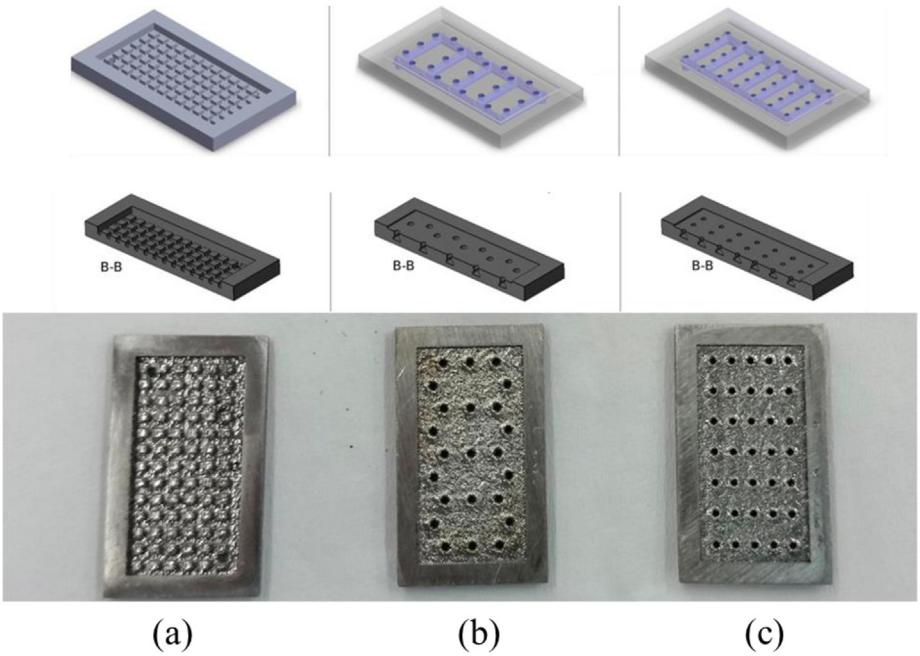

Fig. 10 – 3D-printed micro steel BPPs with (a) open (b) & (c) enclosed flow-fields [97].

Please cite this article as: Baroutaji A et al., Additive manufacturing for Proton Exchange Membrane (PEM) hydrogen technologies: merits, challenges, and prospects, International Journal of Hydrogen Energy, https://doi.org/10.1016/j.ijhydene.2023.07.033

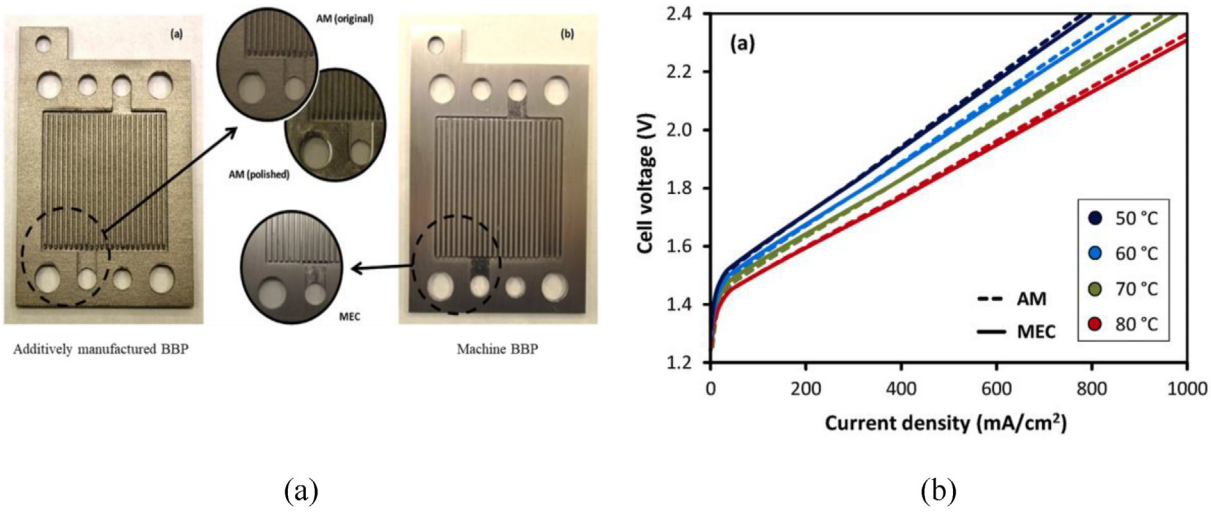

Fig. 11 – The BPPs and test results obtained by Sánchez-Molina et al. [66] (a) SLM and machined BBPs (b) in-situ polarization curves.

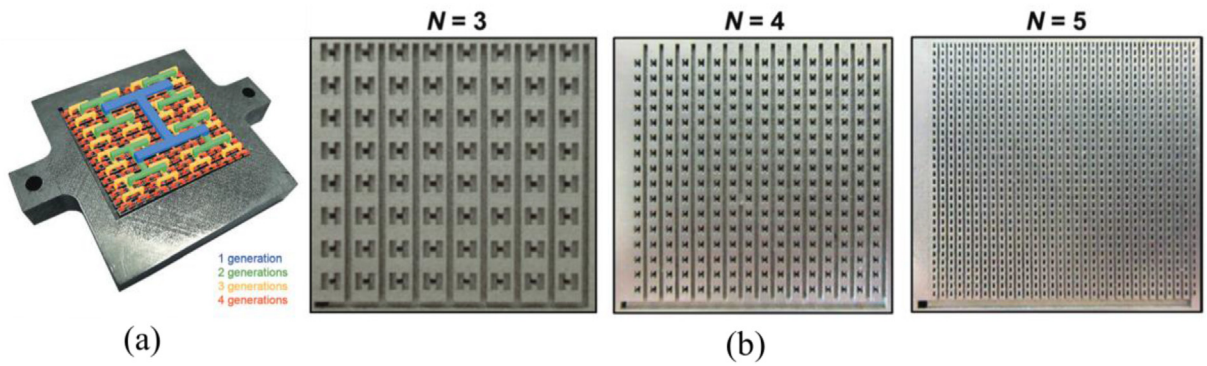

Fig. 12 – Lung-inspired design of BPP (a) explanation of branching generations (b) DMLS-manufactured SS BPPs [98].

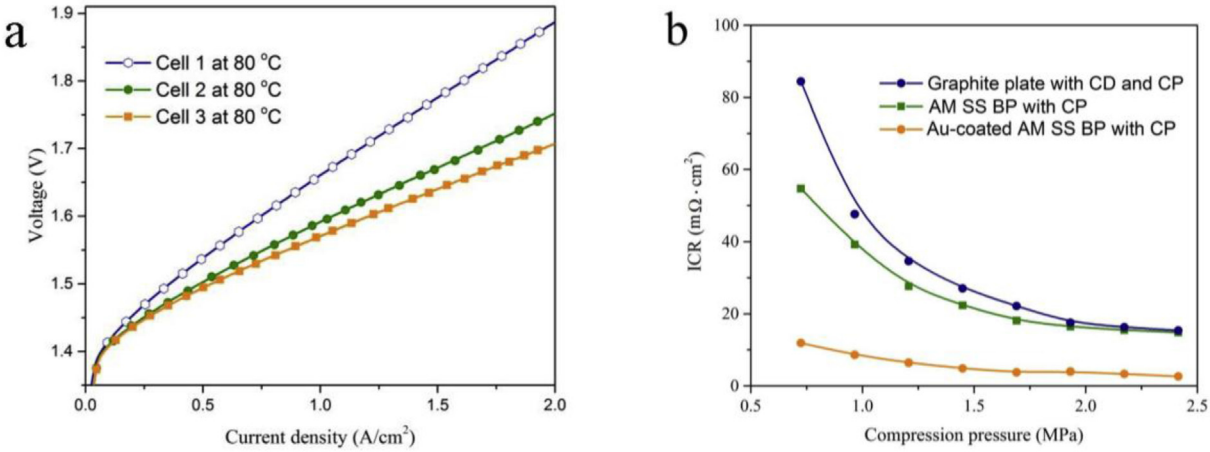

Fig. 13 – (a) Polarization curves and (b) ICR measurements of Au-coated SLM-fabricated SS, bare SLM-fabricated SS, and graphite BBPs [99].

Please cite this article as: Baroutaji A et al., Additive manufacturing for Proton Exchange Membrane (PEM) hydrogen technologies: merits, challenges, and prospects, International Journal of Hydrogen Energy, https://doi.org/10.1016/j.ijhydene.2023.07.033

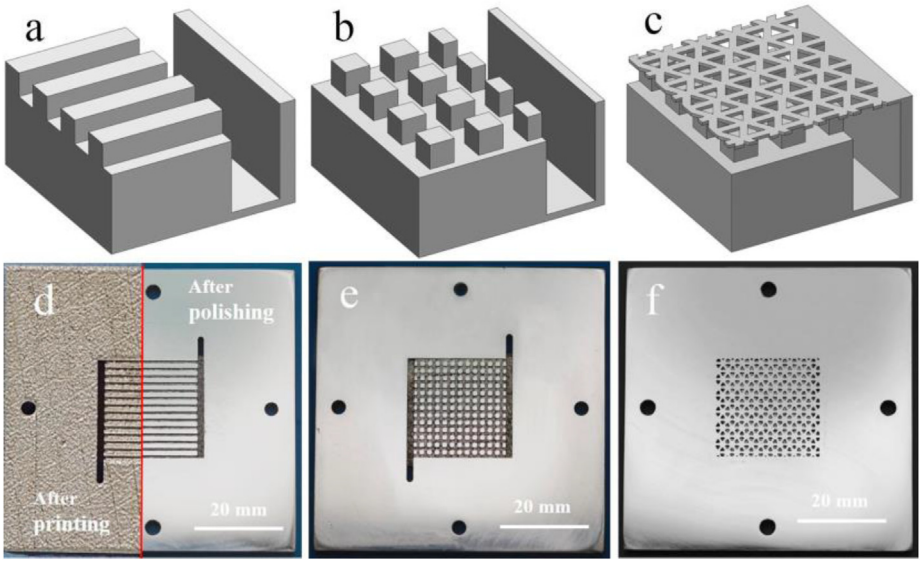

Fig. 14 – Flow-field designs and final 3D-printed plates investigated by Yang et al. [101]: (a) parallel flow-field, (b) pin flow-field, and (c) integrated pin flow-field and GDL, (d) 3D-printed plate with the parallel-flow field, (e) 3D-printed plate with pin flow-field, and (f) 3D-printed integrated plate.

PEMFC stack with 40-cells. It was found that the performance of the single PEMFC with SLSed BPP is similar to that of a standard cell with a carbon flow plate. However, the performance of the PEMFC stack with SLSed BPPs was less than expected due to the inadequate flatness of several BPPs within the stack which in turn increased the overall interfacial contact resistance of the stack.

To utilize the full capability of AM in fabricating advanced parts, Yang et al. [101] proposed an additively manufactured plate as a multifunction plate for the cathode side of PEMWE integrating various parts including BPP, GDL, gasket, and CD. Plates with different flow-field designs including parallel flow-field, pin flow-field, and integrated pin flow-field with GDL, as shown in Fig. 14, were manufactured and compared. SLM was used to fabricate these plates from SS 316 L. Post-SLM polishing of the plates was also used to improve the smoothness of their surfaces. Ex-situ tests were conducted to determine the ohmic resistance while in-situ electrochemical tests were performed to measure the polarization curves and EIS. The results revealed that the integrated plate can reach extremely low ohmic resistance, $\sim 0.1 m\Omega$, compared to other investigated plates. Similarly, the PEMWE with the integrated plate exhibited the highest energy efficiency of 86.48% at 2 A/cm^2. The excellent performance of the integrated plate can be attributed to eliminating the interfacial contact resistances between the matting components, i.e., BPP, GDL, CD, etc.

MEA

IJP was deemed as a suitable AM technique for MEA fabrication because it can deposit inks loaded with solid nanoparticles and therefore it was mainly used for depositing the Pt/C catalyst that has a typical particle size in the range of 100 nm to 1μm [102]. Compared to the other deposition methods, such as screen printing or spray painting, IJP is an attractive technique due to its higher flexibility in patterning, better shape and amount of the released ink, better catalyst utilizations, and ability to produce electrode with very low platinum loading (<0.5 mg Pt cm^{-2}) [50,84]. IJP can facilitate the continuous production of MEA reducing the number of fabrication steps. IJP was successfully used to produce the whole MEA or some of its layers. It was used to deposit the catalyst on either GDL, membrane, or both. It was also utilized to deposit Nafion ionomer onto the catalyst layer through a technique commonly known as direct membrane deposition [103–105].

Shukla et al. [49,106] deposited Pt/C catalyst on Nafion membrane using IJP to create a thin electrode with low platinum loading for both anode and cathode of PEMFC. It was shown through SEM that the ink-jetted CL has a porous structure composed of Pt/C aggregates binded by Nafion ionomer. The fabricated MEA with ink-jetted electrode exhibited better catalyst mass activity than the conventional spray-coated MEA. Towne et al. [83] demonstrated the ability of IJP to fabricate MEA for PEMFC. In this work, a Pt/C catalyst solution was deposited onto the Nafion membrane using a desktop inkjet printer. It was reported that IJP can form a mechanically stable CL with excellent adherence performance without the need for any post-deposition hot-press step. Taylor et al. [50] created an electrode for PEMFC by employing IJP to deposit Pt/C catalyst onto GDL. The fabricated electrodes performed better than their conventionally manufactured counterparts with the same overall platinum loading. Bezerra et al. [107] used IJP to create a double-layer cathode by depositing the catalyst on both carbon GDL and Nafion membrane. Willert et al. [51] adopted IJP to produce three-layers MEA (i.e. CCM) for PEMFC. Three different AM approaches were considered including IJP of the membrane layer

Please cite this article as: Baroutaji A et al., Additive manufacturing for Proton Exchange Membrane (PEM) hydrogen technologies: merits, challenges, and prospects, International Journal of Hydrogen Energy, https://doi.org/10.1016/j.ijhydene.2023.07.033

and the top catalyst layer, IJP of both catalyst layers onto a membrane layer, and finally IJP of the membrane layer as well as the catalyst layers. The 3D-printed MEA exhibited homogeneous Pt-loading and performed better than the conventional MEA achieving 15% higher power density. Cannio et al. [48] used AM microextrusion technique, similar to IJP, to fabricate an electrode, i.e. CL, for PEMFC. In this work, a catalytic ink formed from graphite/water/ethanol suspensions and loaded with platinum, a perfluorosulfonic ionomer, and a pore former (NH_4CO_3) was deposited on GDL. The electrochemical performance of a cell with the 3D-printed catalyst layers was evaluated and compared to that of a standard electrode. The cell with a 3D-printed electrode showed a promising performance with a maximum power density of 727 mW cm^{-2}.

Other relevant parts

The advancement of PEMFC power systems requires not only manufacturing an efficient stack but also developing materials and devices that can produce, store and release hydrogen efficiently. In this context, AM has also been adopted to manufacture different parts relevant to PEMFC power systems such as hydrogen storage materials, hydrogen production reactors, Heat Exchangers (HXs), etc.

For example, Bürger et al. [108] used AM to fabricate a lightweight reactor with high thermal power for preheating of metal hydrides for hydrogen storage and heat recovery applications in PEMFC poly-generation systems. The reactor design was based on tubular heat exchanger geometry, and it was made of aluminium, as shown in Fig. 15.

Lei et al. [109] used AM to fabricate catalyst support for hydrogen production via Methanol Steam Reforming (MSR) micro reactor. The porous catalyst support was fabricated from SS 316 L using SLM. Triply Periodic Minimal Surface (TPMS) with diamond type is utilized to design the pore structure of the catalyst support. TPMS geometry was selected due to its large specific surface area and better interconnectivity. It was found that the hydrogen production performance of MSR with AM catalyst support is better than the reactor with commercial stainless steel catalyst support.

Kreider et al. [110] used FMD to 3D-print a polymer-MOF (Metal Organic Framework) composite of prototypical MOF material (MOF-5) with acrylonitrile butadiene styrene (ABS) for hydrogen storage applications. The hydrogen adsorption and desorption properties of the 3D-printed composite were calculated. The polymer-MOF composite showed better hydrogen adsorption performance than the pure ABS polymer.

The PEMFC power plant uses several HXs to transfer the thermal energy between the hot and the cold streams within the power plant. AM has been used to manufacture different types of HXs. Comprehensive reviews of AM for HXs applications can be found in Refs. [30,38].

Influence of PEM working environment on AMed metals

The metallic materials used in PEMFC and PEMWE are prone to corrosion and Hydrogen Embrittlement (HE) due to the harsh working environment within these systems. The corrosive products, mainly the dissolved metal ions, can contaminate the catalyst sites within MEA and decrease the electrical conductivity of other parts affecting the functionality of the system and reducing its power output [82,111]. Also, the passive layer, formed on the surface of a material, as a result of corrosion, increases ICR reducing the efficiency and electrical output of the system [99]. On the other side, the HE causes significant deterioration of the mechanical properties promoting brittle failure within the metallic part. Therefore, the durability and reliability of AM metals for PEM systems are linked to their corrosion performance and hydrogen embrittlement resistance. Accordingly, in this section, an overview of the relevant literature is given.

Corrosion behaviour of AMed metals

Due to the nature of AM process, the AM-fabricated metals exhibit several unfavourable metallurgical and surface characteristics, such as pores, residual stress, and high surface roughness, which may promote poor corrosion performance. Such inherent characteristics in the AMed parts cannot be eliminated but they can be minimized by selecting the right combination of AM and post-AM processes parameters along with the optimal material composition. The residual stresses are caused by the high thermal gradient due to the local melting and rapid solidification during AM process. Such residual stresses not only cause cracking, warping, and reduced mechanical properties; but may also accelerate both corrosion

Fig. 15 – AM aluminium reactor for preheating of metal hydrides [108].

Please cite this article as: Baroutaji A et al., Additive manufacturing for Proton Exchange Membrane (PEM) hydrogen technologies: merits, challenges, and prospects, International Journal of Hydrogen Energy, https://doi.org/10.1016/j.ijhydene.2023.07.033

attack and stress corrosion cracking [112–114]. Pores are inevitable in AM-fabricated parts due to un-melted powder or the trapped gas in the melting pool or the powder. These pores also form preferred sites for corrosion attack [82]. The surface roughness of AM surfaces is relatively high (~ 10– 30 μm in SLM surfaces) and may accelerate the electrochemical reactions between the AMed part and the surrounding environment leading to both general and localized corrosion. The high surface roughness in AM parts is a result of different sources including, but not limited to, evaporation, balling phenomena, or staircase effects observed during the layer-by-layer building.

The PEM systems have a harsh acidic and humid operating environment which is conducive to corrosion of the metallic parts of the system, particularly BPP and GDL [64,115]. The use of perfluorosulfonic acid polymer, i.e. Nafion, as a membrane in PEM devices creates an acidic environment containing SO_4^{-2}, Cl^- and F^- ions with pH = 2–3 at 70 °C [111,116]. Additionally, the presence of hydrogen at the anode/cathode and the moisture of the membrane increases the acidic conditions [82]. In the corrosion studies, the PEM working environment is normally simulated using sulfuric acid electrolyte solution (0.5 M H_2SO_4) or any similar electrolyte. Further simulation of the anode and cathode environments can be achieved by introducing oxygen and hydrogen bubbles within the electrolyte. The corrosion of AM materials has received extensive research and it has been reviewed in Refs. [82,117,118]. The focus of this section is only on those studies concerned with corrosion responses of AM metals in a PEM-like environment, mainly H_2SO_4 media. Table 2 summarizes the corrosion studies and the main findings.

Lodhi et al. [119] examined the corrosion response of AMed SS 316 L in sulfuric acidic electrolytes with pH in the range of 1–3. The EIS and cyclic polarization (CP) tests were conducted for both AM and wrought samples. For highly acidic environments with pH = 1, the AMed materials exhibited lower corrosion current, i.e., higher corrosion resistance, but higher charge transfer resistance than the conventional wrought material. The good corrosion resistance of AMed materials was due to the forming of fine sub-grains, during the AM process, which in turn enhanced the stability of the passive oxide film formed on the material. It was reported that the passive oxide film generated on the AM material has better barrier characteristics and stability than that formed on wrought materials. Miller et al. [120] investigated the influence of the sulfuric acid environment on SLMed SS 316 L. The SLMed tensile samples were immersed in a solution containing 0.75 M H_2SO_4 for different periods (up to 2184 h) and then the changes in mass and thickness were analysed before conducting the tensile tests. It was found that the AM samples experienced minimal mass loss while their mechanical properties, i.e., tensile stress and strain, decreased after the exposure to sulfuric acid causing brittle failure to these samples. It was reported that HE is the main corrosion form in AM samples. Geenen et al. [121] investigated the corrosion performance of traditional and AMed SS 316 L in 0.5 M H_2SO_4 electrolyte solution. The study considered samples prepared using different fabrication methods including casting, hot isostatic pressing (HIP), SLM and combined SLM with HIP. The SLMed samples were found to show lower corrosion resistance than both the casting and HIP samples. It was reported that the poor corrosion characteristics of the SLMed samples could be caused by the high porosity of these samples. The HIP treatment, used in the combined SLM and HIP fabrication routes, worsen the corrosion performance of the samples as it promoted the spheroidization of the oxides and increased the grain sizes. Kong et al. [116] investigated the influence of heat treatment on the corrosion performance of SLMed SS 316 L for application in BPPs of PEMFC. The acidic working environment of PEMFC was simulated using 0.5 M H_2SO_4 solution with 50 ppm Cl^- and 2 ppm F^- ions. Potentiodynamic and potentiostatic polarization tests were conducted to assess the corrosion behaviour and the stability of the passive film generated on the tested samples. The as-built SLMed samples exhibited a faster corrosion rate than the wrought and heat-treated samples. The poor corrosion resistance of as-built samples was clarified by the SLM-induced defects including the non-equilibrium phases and molten pool boundaries. The recrystallized heat treatment, conducted at a temperate of 1050 °C for 30 min, was reported to improve the corrosion performance due to its ability to generate a uniform structure and thicker passive film on the samples. In another study, Kong et al. [122] compared the corrosion resistance properties of SLMed and wrought SS 316 L. It was found that SLMed material exhibited minimal transformation of austenite into martensite and therefore it has better durability and less damage in a hydrogen environment than the wrought material. Also, it was observed that the SLMed material showed a lower corrosion rate, i.e., higher corrosion resistance, than the wrought counterparts in the hydrogen-charged environment. This study confirmed the suitability of SLMed SS 316 L to manufacture parts for use in PEMFC. Yang et al. [99] compared the corrosion responses of bare and gold-coated (Au-coated) SLMed SS 316 L. H_2SO_4 solution with pH = 2 and bubbled with O_2 was used as an electrolyte to simulate the anodic environment of PEMWE. The potentiodynamic and potentiostatic curves were recorded and used to evaluate the corrosion properties. It was reported that the Au-coated samples showed remarkable corrosion resistance which is much higher than that of the bare samples. Sánchez-Molina et al. [66] examined the corrosion performance of SLMed SS 316 L in a PEMWE ambient (simulated using 0.1 M $NaHSO_4$+5 ppm hydrofluoric acid (HF)) and compared it with that of conventionally machined material. Both the SLMed and conventional materials exhibited comparable corrosion behaviour in terms of corrosion potential and current density values, as shown in Fig. 16. Svendby et al. [123] fabricated Inconel 625 samples using SLM for BPP applications in HT-PEMFC. Post-AM machining was used to produce surface roughness of ~ 0.3 μm. The fabricated samples were tested for their ICR and anti-corrosive properties in a HT-PEMFC simulated environment. Concentrated unaltered phosphoric acid (85% H_3PO_4) purged with nitrogen (N_2) for 30 min was used as an electrolyte for the corrosion tests. The performance of the AM samples was compared against traditional hot-rolled samples. The AMed samples exhibited higher corrosion rates and lower ICR values than the hot-rolled samples. The authors reported that additional work is still needed to produce AMed BPP with desirable properties. Cheng et al. [124] studied the influence of heat treatment on

Please cite this article as: Baroutaji A et al., Additive manufacturing for Proton Exchange Membrane (PEM) hydrogen technologies: merits, challenges, and prospects, International Journal of Hydrogen Energy, https://doi.org/10.1016/j.ijhydene.2023.07.033

Table 2 – Summary of studies on corrosion performance of AMed metals in PEM working environment.

Material	AM method	Heat treatment	Coating	Environment	Corrosion characterization	Other important measurements	Material and microstructure characterization	Counterparts used for comparison	Main findings	Ref
Inconel 625	SLM	None	None	HT-PEMFC environment (85% H_3PO_4)	Potentiodynamic and potentiostatic polarization	ICR	SEM	SLMed and commercial materials	SLMed materials have a higher corrosion rate than commercial materials. Post-corrosion ICR of commercial materials is greater than that of SLMed materials.	[123]
SS 316L	SLM	None	None	H_2SO_4 with and without CL^- (pH = 1 to 3)	Potentiodynamic polarization	EIS	EDX, XRD, XSP, SEM	SLM-fabricated and wrought materials	SLM-fabricated material has higher corrosion resistance but higher charge transfer resistance than the wrought material	[119]
SS 316L	SLM	None	None	0.5 M H_2SO_4 purged with nitrogen	Potentiodynamic polarization		OM, SEM, EDS	SLMed, cast, and HIP materials	SLM material has lower corrosion resistance than both the casting and HIP material	[121]
SS 316L	SLM	HT1: Temperature = 650 °C, Duration = 30 min HT2: Temperature = 1050 °C, Duration = 30 min	None	PEMFC environment (0.5 M H_2SO_4 solution + 50 ppm Cl^- + 2 ppm F^- ions)	Potentiodynamic and potentiostatic polarization		EBSD, TEM, EDS, XPS, ICP-MS	As built and heat-treated SLM materials	• The as-built SLM-fabricated material has a faster corrosion rate than the wrought and heat-treated material • Heat treatment can improve the corrosion performance • The current densities for the as-built SLMed and HT1-treated SLMed 316 L were higher than the DOE 2020 target.	[116]
SS 316L	SLM	None	None	PEMFC environment (0.5 M H_2SO_4 solution + 50 ppm Cl^- + 2 ppm F^- ions)	Potentiodynamic and potentiostatic polarization	EIS	EBSD, XRD	SLMed and wrought materials	• SLM material has higher corrosion resistance than wrought material in the hydrogen-charged environment. • The current densities of the hydrogen-charged SLMed material met the DOE while the wrought material did not.	[122]
SS 316L	SLM	None	Au	$H_2SO_4 + O_2$ bubbles (pH = 2)	Potentiodynamic and potentiostatic polarization	ICR, in-situ polarization and EIS	XRD, SEM	Coated and bare SLM-fabricated materials	Coated materials showed remarkable corrosion resistance compared to bare materials	[99]
SS 316L	SLM	None	None	PEMFC environment (0.1 M $NaHSO_4$+5 ppm HF)	Potentiodynamic polarization		SEM, EDS	SLMed and machined materials	Machined and SLMed materials showed similar corrosion responses.	[66]

(*continued on next page*)

Table 2 – (continued)

Material	AM method	Heat treatment	Coating	Environment	Corrosion characterization	Other important measurements	Material and microstructure characterization	Counterparts used for comparison	Main findings	Ref
CoCrFeMnNi HEA	SLM	HT1: Temperature = 600 °C, Duration = 30 min HT2: Temperature = 800 °C, Duration = 30 min HT3: Temperature = 1000 °C, Duration = 30 min	None	PEMFC environment (0.5 M H_2SO_4 solution + 5 ppm F^- ions+ air bubbles)	Potentiodynamic and potentiostatic polarization		XRD, EBSD, ECCI, TEM, EDS	As built and heat-treated SLMed materials	• The heat-treated samples have better corrosion resistance than the as-built samples. • The heat treatment at 1000 °C, i.e., HT3, provides the best passive stability and the highest corrosion resistance among all the investigated heat treatment protocols.	[124]

Optical microscopy (OM), Scanning electron microscopy (SEM), X-ray diffraction (XRD), electron back-scattered diffraction (EBSD), electron channelling contrast imaging (ECCI), transmission electron microscopy (TEM), energy dispersive spectroscopy (EDS), X-ray photoelectron spectroscopy (XPS), inductively coupled plasma mass spectrometry (ICP-MS).

the corrosion performance of SLMed CoCrFeMnNi high entropy alloy (HEA) in the simulated PEMFC environment. It was found that the high treatment temperature can homogenize the composition and distribution of the HEA substructure, prevent the depletion of Cr at grains boundaries, and enhance the overall corrosion resistance.

Hydrogen embrittlement of AMed metals

HE, or Hydrogen-Induced Cracking (HIC), is the degradation of the mechanical properties of metals due to hydrogen. The presence of hydrogen in metallic materials and alloys can reduce the ductility and strength leading to transition from desirable ductile failure to brittle fracture mode [125]. It is believed that HE is caused by the diffusion of hydrogen, i.e., entry of hydrogen atoms, into the metal lattice and accumulation near dislocation sites or microvoids [126]. The diffused hydrogen creates brittle carbide and hydride precipitates within the metals that negatively affect the mechanical properties [120]. In the HE investigations, the material samples are exposed to hydrogen for some time before examining their mechanical properties. HE of AMed metals has received limited studies in the literature, a summary of these studies is presented in Table 3.

Bertsch et al. [125] studied the HE behaviour of AM SS 316 L manufactured by SLM and DED. As-built and heat-treated tensile samples were used in this work. It was found that hydrogen reduced the ductility in as-built DED material but did not affect the tensile properties of SLMed or heat-treated materials. The close inspection of the microstructures suggested that hydrogen increased the void area within all investigated materials. Also, it was proposed that the initial microstructure in terms of morphology and spacing of dislocations play a significant role in the material response to hydrogen. It was reported that SLMed materials are more suitable for use in hydrogen environments compared to DED materials. Baek et al. [127] examined the resistance to HE in additively manufactured SS 304 L and compared it with conventional rolled material. DED was proposed as AM method and used to fabricate the tensile test specimens. The specimens were charged with hydrogen gas for 5 days at 10 MPa and 150 °C before conducting the tensile tests. According to the results presented in Fig. 17, the hydrogen had a minimal influence on AMed samples while it greatly affected the rolled samples by reducing their toughness. Such results indicate that the AMed samples have higher HE resistance than the rolled counterparts which makes them suitable to be adopted in hydrogen-based technology such as PEMFC and PEMWE.

Lee et al. [128] compared the HE resistance of SLMed SS 304 L to that of conventionally manufactured material. Two different conventional processing routes were considered including cast and annealed (CA); and cast, annealed and thermomechanical treatment (CA-TMT). According to the findings of this study, the SLMed and CA-TMT samples exhibited higher HE resistance than the CA samples. The good HE behaviour of the SLMed material was rationalised by the features of its microstructure including the full austenitic structure and homogeneous distributions of its constituent elements. Silverstein and Eliezer [129] examined the hydrogen trapping mechanisms and hydrogen desorption behaviour of

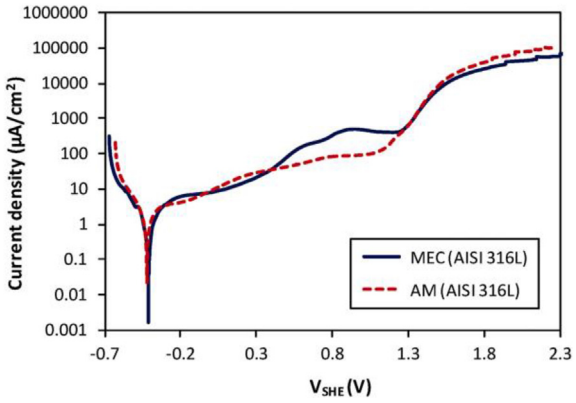

Fig. 16 – Potentiodynamic polarization of SLM conventionally machined 316 L SS [66].

3D printed Ti–6Al–4V. SLM with different building directions was used to fabricate the different samples for this study. The fabricated titanium parts were charged with hydrogen gas for 10 h at pressure and temperature of 0.5 MPa and 500 °C, respectively. The hydrogen desorption behaviour was assessed using Thermal Desorption Spectrometry (TDS). It was found that the AM printing direction influences the hydrogen desorption characteristics and the susceptibility to hydrogen embrittlement. Such influence is because the different building orientations yield different microstructural changes and metal defects which in turn affect the hydride content and the amount of trapping energy.

Merits, challenges, and prospects of AM for PEM fabrication

As a digital manufacturing method, AM is an attractive option for PEM fabrication because it can speed up the development cycle through rapid prototyping of new and testable designs without the need for costly tooling [100]. AM can produce PEM components with intricate 3D geometry, sometimes required for enhancing the electrochemical activities and mass transport performance of the part, with lower labour and cost compared to CM methods [130]. The diversity of the materials suitable for AM and the capability to mix new alloys is another advantage to produce functioning components with appropriate characterises for PEM devices [40]. AM is also an important solution for the PEM systems that will be deployed in remote and hard-to-reach areas, such as space, aircraft carriers, submarines, etc., as they enable on-demand manufacturing and onsite fabrication of parts reducing the reliance on the unreliable supply chain in such sites [66]. AM can be used not only to manufacture the main components of the PEM devices but also to produce parts of relevant technologies such as hydrogen production reactors, hydrogen storage materials, and heat transfer surfaces. Fig. 18 shows the AM techniques used to fabricate the different parts of PEM devices.

PBF techniques, mainly SLM and SLS, were used to fabricate BPP and GDL. Such techniques provide great design freedom to manufacture highly complex flow-field configurations with optimized performance enabling uniform distribution of the reactants, minimum pressure drop, and low contact resistance. PBF methods can simplify the production route of BPP and GDL as the parts are readily generated from 3D-CAD designs with little post-processing requirements and less material waste. They are also beneficial to produce one integrated multifunctional part with internal flow channels combining multiple components such as BPP, GDL, and CP [40,101]. However, PBF techniques are relatively slow compared to CM methods, used in BPP and GDL fabrication, forming a major obstacle towards adopting AM for mass production of such parts.

IJP has been extensively used in fabricating MEA where thin layers of the membrane, catalysts, or both were deposited over conventional substrates. The deposition capability of IJP has been progressively extended from single-layer to multilayers which enabled the manufacturing of a whole functional MEA continuously without the need for multiple steps. However, IJP is a simple layer deposition method and cannot fabricate complex geometry, therefore, the use of IJP was limited to MEA with a simple structure [131]. The beneficial effects of increasing shape and hierarchical complexity in some MEA layers, such as catalyst support structure, are limited in IJP and only achievable if another AM method, such as SLM, is used in conjunction with IJP.

Despite the huge potential, AM still faces some challenges for PEMFC and PEMWE manufacturing. The AMed parts are prone to geometrical defects that might lead to deviations between the designed and manufactured dimensions. Such deviation may influence the function of the part as well as its alignment and contact with the other PEM parts resulting in unfavourable behaviour such as poor mass transport and high contact resistance. Therefore, a comprehensive dimensional analysis should be conducted on the AMed PEM components using advanced measurement equipment, such as Coordinate Measuring Machine (CMM), in order to ensure their dimensional accuracy and minimize the influence of the geometrical defects on the functional performance of the parts.

The durability of the AM-fabricated metals is also a major concern due to corrosion. The metallurgical defects of the AMed materials, such as residual stresses, porosity, inclusion, and rough surfaces, form sites for corrosion attack. The corrosion performance of additively manufactured metals, such as stainless steel, has received considerable attention in the literature. However, only limited work studied the corrosion of AMed stainless steel in the PEM working environment, i.e., acidic media with pH of 2–3 and hydrogen/oxygen gas bubbles. Similarly, there is limited information about the corrosion of other AM metals, such as Al and Ti alloys, in the PEM environment. Therefore, more research work is still needed to fully understand the corrosion of AMed materials and to identify their suitability for PEM devices. The recent advancements in AM showed the capability to fabricate materials with high corrosion resistance, such as copper (Cu) and silver (Ag). For example, SLM has been used successfully to fabricate Cu and Ag-based alloys for different applications [132]. Thus, alloying such materials with the traditional

Please cite this article as: Baroutaji A et al., Additive manufacturing for Proton Exchange Membrane (PEM) hydrogen technologies: merits, challenges, and prospects, International Journal of Hydrogen Energy, https://doi.org/10.1016/j.ijhydene.2023.07.033

Table 3 – Summary of studies on HE performance of AMed metals.

AM material	AM method	Heat treatment	Counterparts used for comparison	Hydrogen charging conditions	Main experimental work	Main findings	Ref
S 316L	SLM & DED	Temperature = 1000 °C, Duration = 1 h followed by water quench	As-built and heat-treated AM-materials	Materials were charged with hydrogen gas for 400 h at 120 MPa and 280 °C.	• Tensile testing was used to evaluate the mechanical properties. • Microstructural analysis.	SLMed materials are better than DED materials for hydrogen applications.	[125]
SS 304L	DMT	None	SLMed and rolled material	Materials were charged with hydrogen gas for 5 days at 10 MPa and 150 °C	• Tensile testing was used to evaluate the mechanical properties. • TDS was used to analyse the hydrogen evolution characteristics. • Microstructural analysis.	SLMed materials have better HE resistance than the rolled material.	[127]
SS 304L	SLM	None	SLMed, cast and annealed (CA); and cast, annealed and thermomechanical treatment (CA-TMT).	Electrochemical hydrogen charging was conducted in 2 g/L CH_4N_2S in 0.5 M H_2SO_4 solution at room temperature for up to five days.	• Tensile testing was used to evaluate the mechanical properties. • TDS was used to analyse the hydrogen desorption behaviour • Microstructural analysis.	SLMed and CA-TMT materials have higher HE resistance than the CA material.	[128]
Ti–6Al–4V	SLM	None	SLMed material only	Material charged with hydrogen gas for 10 h at 0.5 MPa and 500 °C	• TDS was used to evaluate the hydrogen desorption characteristics. • Microstructural analysis.	The AM building direction has an influence on hydrogen desorption characteristics and the susceptibility to hydrogen embrittlement.	[129]

Thermal Desorption Spectrometry (TDS).

Please cite this article as: Baroutaji A et al., Additive manufacturing for Proton Exchange Membrane (PEM) hydrogen technologies: merits, challenges, and prospects, International Journal of Hydrogen Energy, https://doi.org/10.1016/j.ijhydene.2023.07.033

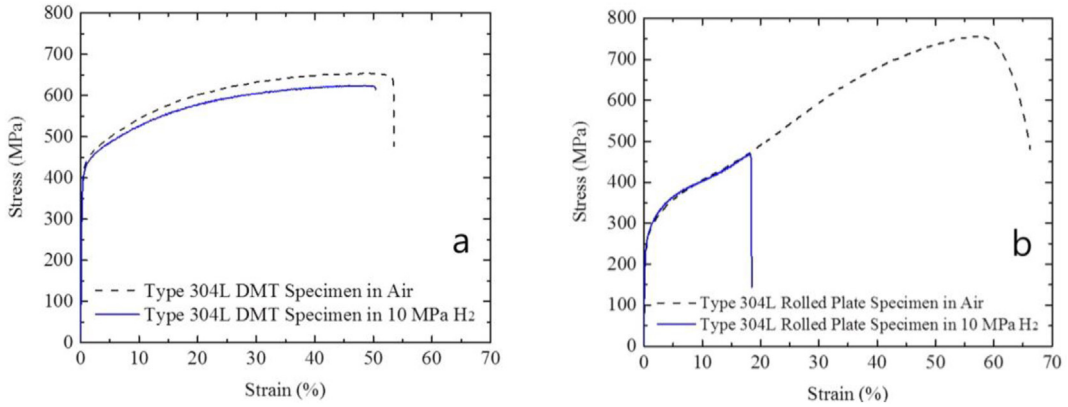

Fig. 17 – The stress-strain curves of (a) AM and (b) rolled 304 L SS showing the influence of hydrogen on the mechanical responses [111].

metals used in PEM parts and processing them via AM is expected to attract attention in future research to improve the corrosion performance of AMed metals.

The hydrogen embrittlement phenomenon is another cause of durability concern for AMed materials used in PEM systems. To date, the HE of AMed materials have received limited research investigations and therefore further work is still needed in this area to identify the potential failure mechanisms and establish the required safety regimes for using AMed metallic materials in hydrogen technologies.

The metallurgical properties, which affect the corrosion and HE performance, of the AM materials depend on different factors including feedstock properties, printing parameters, and post-printing processes. Applying the right sets and optimal parameters is crucial for creating a functional PEM component. However, there is a lack of systematic optimization analysis for each AM material suitable for PEM applications and therefore this can be another dimension for future research.

Among the promising applications of AM is the capability to produce High Entropy Alloys (HEAs) [133]. HEAs are excellent candidates for hydrogen energy technologies as they have promising electrocatalytic performance and hydrogen storage properties [134,135]. Some HEAs, such as np-HEA, have exhibited excellent mass activity for Oxygen Reduction Reaction (ORR) which is ten times better than Pt/C catalyst [136]. Similarly, the Body-Centred Cubic (BCC) HEAs showed superior hydrogen storage capacity compared to conventional BCC alloys [134]. The AM of those HEAs suitable for PEM devices received limited attention in the literature and therefore this area could be an important field for future research investigations.

The technical suitability of new materials/components for PEM systems is normally evaluated by checking whether they meet the up-to-date and relevant US Department of Engineering (DOE) technical targets. Limited attempts were made in the literature to compare the performance of AMed components with the DOE targets therefore further research is still needed in this area to verify the technical suitability of such components and ensure their competitiveness for future PEM systems.

The one-step continuous manufacturing process is highly desirable to enhance the production efficiency of PEM components. The capability of multi-materials printing is important to enable the continuous manufacturing of some PEM parts such as MEA and BPP with an anti-corrosion layer. The multi-material capability varies among the different AM methods where it is relatively good using IJP but it is quite challenging in PBF technologies [18]. Expanding the multi-material capabilities of commercial AM systems should enable the efficient 3D printing of the whole PEM devices.

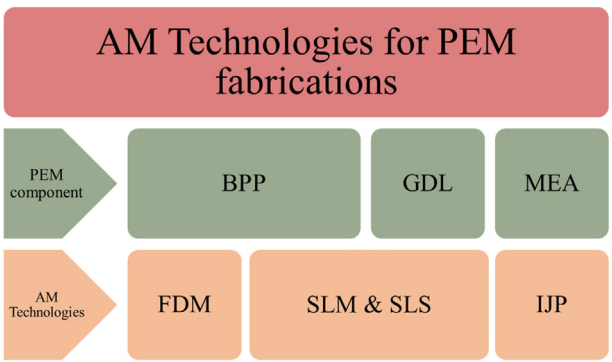

Fig. 18 – AM methods used for each PEM component.

Conclusion

In this paper, a thorough review of additively manufactured parts for PEM systems is conducted. The paper also presents an assessment of the studies on corrosion and hydrogen embrittlement performance of additively manufactured materials in the PEM working environment. Additionally, the major drawbacks of AM techniques in fabricating PEM components are summarized and possible solutions are suggested along with future research directions.

AM technologies have the potential to revolutionize the fabrication process of advanced PEM systems. The capability

Please cite this article as: Baroutaji A et al., Additive manufacturing for Proton Exchange Membrane (PEM) hydrogen technologies: merits, challenges, and prospects, International Journal of Hydrogen Energy, https://doi.org/10.1016/j.ijhydene.2023.07.033

of AM methods to fabricate parts with greater shape complexity that outperform conventional shapes enable solving different problems within the device such as high contact resistance, poor mass and heat transport, etc. Leading to enhanced performance. AM technologies are particularly beneficial for fabricating PEM components with internal channels or porous structures, such as BPP and GDL, that are difficult and costly to be obtained by conventional machining. IJP and SLM are the most promising AM techniques for fabricating PEM components. IJP is used for MEA fabrication while SLM is adopted for BPPs and GDLs.

Despite their potential, the additively manufactured metallic parts still require significant improvement before they can be considered as reliable materials for PEM applications. The surface roughness, residual stresses, and pores within AMed metals increase their corrosion rate. Therefore, the printing and post-printing process parameters should be optimized to produce parts with minimum metallurgical defects to ensure adequate mechanical and corrosion performance.

To date, 3D-printing of a full operational PEM device in one additive manufacturing system is not possible since different materials and different AM processes are required for the different parts of the device. Releasing the full potential of AM for PEM applications requires; expanding the multi-material capability of AM system; as well as increasing the portfolio of the printable functional materials; to allow 3DP of the different PEM parts.

In summary, using AM for PEM fabrication is an important step to increase the manufacturing readiness level of the technologies so they meet the commercialization cost targets. As a digital manufacturing technique, AM is an important ingredient in the Industry 4.0 era and can contribute to the digitalization of PEM production. AM still suffers some limitations centred around slow build speed, limited material options, and inefficiency for mass production. However, it is predicted that the huge and dramatic developments taking place currently in AM technologies will mitigate such problems in the near future and this will lead eventually to more adoption of AM-fabricated parts in the PEM industry.

Declaration of competing interest

The authors declare that they have no known competing financial interests or personal relationships that could have appeared to influence the work reported in this paper.

REFERENCES

[1] Alaswad A, et al. Technical and commercial challenges of proton-exchange membrane (PEM) fuel cells. Energies Dec. 2020;14(1):144. https://doi.org/10.3390/en14010144. 2020, Vol. 14, Page 144.

[2] Baroutaji A, Carton JG, Stokes J, Olabi AG. Application of open pore cellular foam for air breathing PEM fuel cell. Int J Hydrogen Energy Oct. 2017;42(40):25630–8. https://doi.org/10.1016/j.ijhydene.2017.05.114.

[3] Sayed ET, et al. Augmenting performance of fuel cells using nanofluids. Therm Sci Eng Prog Jul. 2021:101012. https://doi.org/10.1016/J.TSEP.2021.101012.

[4] van Biert L, Godjevac M, Visser K, Aravind PV. A review of fuel cell systems for maritime applications. J Power Sources Sep. 30, 2016;327:345–64. https://doi.org/10.1016/j.jpowsour.2016.07.007. Elsevier B.V.

[5] Xing H, Stuart C, Spence S, Chen H. Fuel cell power systems for maritime applications: progress and perspectives. Sustain Times Jan. 2021;13(3):1213. https://doi.org/10.3390/SU13031213. 2021, Vol. 13, Page 1213.

[6] Wilberforce T, et al. Developments of electric cars and fuel cell hydrogen electric cars. Int J Hydrogen Energy 2017;42(40):25695–734. Accessed: May 05, 2018. [Online]. Available: http://linkinghub.elsevier.com/retrieve/pii/S036031991732791X.

[7] Baroutaji A, Wilberforce T, Ramadan M, Olabi AG. Comprehensive investigation on hydrogen and fuel cell technology in the aviation and aerospace sectors. Renew Sustain Energy Rev May 2019;106:31–40. https://doi.org/10.1016/J.RSER.2019.02.022.

[8] Paul B, Andrews J. PEM unitised reversible/regenerative hydrogen fuel cell systems: state of the art and technical challenges. In: Renewable and sustainable energy reviews, 79. Elsevier Ltd; Nov. 01, 2017. p. 585–99. https://doi.org/10.1016/j.rser.2017.05.112.

[9] Kundu PP, Dutta K. Hydrogen fuel cells for portable applications. In: Ball M, Basile A, Veziroğlu TN, editors. Compendium of hydrogen energy. Oxford: Woodhead Publishing; 2016. p. 111–31. https://doi.org/10.1016/B978-1-78242-364-5.00006-3.

[10] Elmer T, Worall M, Wu S, Riffat SB. In: Fuel cell technology for domestic built environment applications: state of-the-art review, 42. Elsevier Ltd; 2015. p. 913–31. https://doi.org/10.1016/j.rser.2014.10.080.

[11] Baroutaji A, Arjunan A, Robinson J, Wilberforce T, Abdelkareem MA, Olabi AG. PEMFC poly-generation systems: developments, merits, and challenges. Sustain Times Oct. 2021;13(21):11696. https://doi.org/10.3390/SU132111696. 2021, Vol. 13, Page 11696.

[12] Staffell I, et al. The role of hydrogen and fuel cells in the global energy system. Energy Environ Sci 2019. https://doi.org/10.1039/C8EE01157E.

[13] Olabi AG, et al. Large-vscale hydrogen production and storage technologies: current status and future directions. Int J Hydrogen Energy Jul. 2021;46(45):23498–528. https://doi.org/10.1016/J.IJHYDENE.2020.10.110.

[14] Bičáková O, Straka P. Production of hydrogen from renewable resources and its effectiveness. Int J Hydrogen Energy Aug. 2012;37(16):11563–78. https://doi.org/10.1016/J.IJHYDENE.2012.05.047.

[15] Shiva Kumar S, Himabindu V. Hydrogen production by PEM water electrolysis – a review. Materials Science for Energy Technologies Dec. 01, 2019;2(3):442–54. https://doi.org/10.1016/j.mset.2019.03.002. KeAi Communications Co.

[16] Wang J, Wang H, Fan Y. Techno-economic challenges of fuel cell commercialization. Engineering Jun. 2018;4(3):352–60. https://doi.org/10.1016/J.ENG.2018.05.007.

[17] Chen Z, Zuo W, Zhou K, Li Q, Huang Y, J. E. Multi-objective optimization of proton exchange membrane fuel cells by RSM and NSGA-II. Energy Convers Manag Feb. 2023;277:116691. https://doi.org/10.1016/j.enconman.2023.116691. Accessed: May 09, 2023. [Online]. Available:.

[18] Human G, van Schoor G, Uren KR. Genetic fuzzy rule extraction for optimised sizing and control of hybrid renewable energy hydrogen systems. Int J Hydrogen Energy

Please cite this article as: Baroutaji A et al., Additive manufacturing for Proton Exchange Membrane (PEM) hydrogen technologies: merits, challenges, and prospects, International Journal of Hydrogen Energy, https://doi.org/10.1016/j.ijhydene.2023.07.033

Jan. 2023;46(5):3576–94. Accessed: May 09, 2023. [Online]. Available: www.sciencedirect.com.
[19] Liu S, Tan J, Hu H, Lu C, Xuan D. Multi-objective optimization of proton exchange membrane fuel cell geometry and operating parameters based on three new performance evaluation indexes. Energy Convers Manag 2023;277:116642. https://doi.org/10.1016/j.enconman.2022.116642.
[20] Kampker A, et al. Challenges towards large-scale fuel cell production: results of an expert assessment study. Int J Hydrogen Energy Oct. 2020;45(53):29288–96. https://doi.org/10.1016/j.ijhydene.2020.07.180. Accessed: May 16, 2023. [Online]. Available:.
[21] Zhang F, et al. 3D printing technologies for electrochemical energy storage. Nano Energy Oct. 01, 2017;40:418–31. https://doi.org/10.1016/j.nanoen.2017.08.037. Elsevier Ltd.
[22] Javaid M, Haleem A, Singh RP, Suman R, Rab S. Role of additive manufacturing applications towards environmental sustainability. Adv. Ind. Eng. Polym. Res. Oct. 2021;4(4):312–22. https://doi.org/10.1016/J.AIEPR.2021.07.005.
[23] Baroutaji A, Arjunan A, Singh G, Robinson J. Crushing and energy absorption properties of additively manufactured concave thin-walled tubes. Results Eng Jun. 2022;14:100424. https://doi.org/10.1016/J.RINENG.2022.100424.
[24] Peng T, Kellens K, Tang R, Chen C, Chen G. Additive manufacturing. Sustainability of additive manufacturing: An overview on its energy demand and environmental impact May 01, 2018;21:694–704. https://doi.org/10.1016/j.addma.2018.04.022. Elsevier B.V.
[25] Colorado HA, Velásquez EIG, Monteiro SN. Sustainability of additive manufacturing: the circular economy of materials and environmental perspectives. J Mater Res Technol Jul. 2020;9(4):8221–34. https://doi.org/10.1016/J.JMRT.2020.04.062.
[26] Blakey-Milner B, et al. Metal additive manufacturing in aerospace: a review. Mater Des Nov. 2021;209:110008. https://doi.org/10.1016/J.MATDES.2021.110008.
[27] Charles A, Hofer A, Elkaseer A, Scholz SG. Additive manufacturing in the automotive industry and the potential for driving the green and electric transition. Smart Innov. Syst. Technol. 2022;262:339–46. https://doi.org/10.1007/978-981-16-6128-0_32/COVER. SIST.
[28] Kumar R, Kumar M, Chohan JS. The role of additive manufacturing for biomedical applications: A critical review 2021;64:828–50.
[29] Chhaya MP, Poh PSP, Balmayor ER, Van Griensven M, Schantz JT, Hutmacher DW. 10.1586/17434440.2015.1059274. In: Additive manufacturing in biomedical sciences and the need for definitions and norms, 12; Sep. 2015. p. 537–43. https://doi.org/10.1586/17434440.2015.1059274. 5.
[30] Kaur I, Singh P. State-of-the-art in heat exchanger additive manufacturing. Int J Heat Mass Tran Oct. 01, 2021;178. https://doi.org/10.1016/j.ijheatmasstransfer.2021.121600. Elsevier Ltd.
[31] Delgado Camacho D, et al. Applications of additive manufacturing in the construction industry – a forward-looking review. Autom ConStruct May 2018;89:110–9. https://doi.org/10.1016/j.autcon.2017.12.031. Accessed: May 17, 2023. [Online]. Available:.
[32] Yap YL, Yeong WY. Additive manufacture of fashion and jewellery products: a mini review. Virtual Phys Prototyp 2014;9(3):195–201. https://doi.org/10.1080/17452759.2014.938993.
[33] Ambrosi A, Moo JGS, Pumera M. Helical 3D-printed metal electrodes as custom-shaped 3D platform for electrochemical devices. Adv Funct Mater Feb. 2016;26(5):698–703. https://doi.org/10.1002/ADFM.201503902.
[34] Hashemi SMH, Babic U, Hadikhani P, Psaltis D. The potentials of additive manufacturing for mass production of electrochemical energy systems. Curr. Opin. Electrochem. Apr. 2020;20:54–9. https://doi.org/10.1016/J.COELEC.2020.02.008.
[35] Sun C, Wang Y, McMurtrey MD, Jerred ND, Liou F, Li J. Additive manufacturing for energy: a review. Appl Energy Jan. 2021;282:116041. https://doi.org/10.1016/J.APENERGY.2020.116041.
[36] Gulzar U, Glynn C, O'Dwyer C. Additive manufacturing for energy storage: methods, designs and material selection for customizable 3D printed batteries and supercapacitors. In: Current opinion in electrochemistry, 20. Elsevier B.V.; Apr. 01, 2020. p. 46–53. https://doi.org/10.1016/j.coelec.2020.02.009.
[37] Zhakeyev A, Wang P, Zhang L, Shu W, Wang H, Xuan J. Additive manufacturing: unlocking the evolution of energy materials. Adv Sci Oct. 2017;4(10). https://doi.org/10.1002/ADVS.201700187.
[38] Jafari D, Wits WW. The utilization of selective laser melting technology on heat transfer devices for thermal energy conversion applications: a review. In: Renewable and sustainable energy reviews, 91. Elsevier Ltd; Aug. 01, 2018. p. 420–42. https://doi.org/10.1016/j.rser.2018.03.109.
[39] Pang Y, et al. Additive manufacturing of batteries. Adv Funct Mater Jan. 2020;30(1):1906244. https://doi.org/10.1002/ADFM.201906244.
[40] Zhang C, Wang S, Li J, Zhu Y, Peng T, Yang H. Additive manufacturing of products with functional fluid channels: a review. Addit Manuf Dec. 2020;36:101490. https://doi.org/10.1016/j.addma.2020.101490.
[41] Laguna OH, Lietor PF, Godino FJI, Corpas-Iglesias FA. A review on additive manufacturing and materials for catalytic applications: milestones, key concepts, advances and perspectives. Mater Des Oct. 2021;208:109927. https://doi.org/10.1016/J.MATDES.2021.109927.
[42] Ryan KR, Down MP, Hurst NJ, Keefe EM, Banks CE. Additive manufacturing (3D printing) of electrically conductive polymers and polymer nanocomposites and their applications. eScience; Aug. 2022. https://doi.org/10.1016/J.ESCI.2022.07.003.
[43] Parra-Cabrera C, Achille C, Kuhn S, Ameloot R. 3D printing in chemical engineering and catalytic technology: structured catalysts, mixers and reactors. Chem Soc Rev Jan. 2018;47(1):209–30. https://doi.org/10.1039/C7CS00631D.
[44] Rasaki SA, Liu C, Lao C, Zhang H, Chen Z. The innovative contribution of additive manufacturing towards revolutionizing fuel cell fabrication for clean energy generation: a comprehensive review. In: Renewable and sustainable energy reviews, 148. Elsevier Ltd; Sep. 01, 2021. https://doi.org/10.1016/j.rser.2021.111369.
[45] Badgett A, Ruth M, Pivovar B. Economic considerations for hydrogen production with a focus on polymer electrolyte membrane electrolysis. Electrochem. Power Sources Fundam. Syst. Appl. Hydrog. Prod. by Water Electrolysis Jan. 2022:327–64. https://doi.org/10.1016/B978-0-12-819424-9.00005-7.
[46] Ahmad S, Nawaz T, Ali A, Orhan MF, Samreen A, Kannan AM. An overview of proton exchange membranes for fuel cells: materials and manufacturing. Int J Hydrogen Energy May 22, 2022;47(44):19086–131. https://doi.org/10.1016/j.ijhydene.2022.04.099. Elsevier Ltd.
[47] Baroutaji A, et al. Materials for fuel cell membranes. In: Encyclopedia of smart materials. Elsevier; 2021. p. 267–72. https://doi.org/10.1016/B978-0-12-815732-9.00034-6.

Please cite this article as: Baroutaji A et al., Additive manufacturing for Proton Exchange Membrane (PEM) hydrogen technologies: merits, challenges, and prospects, International Journal of Hydrogen Energy, https://doi.org/10.1016/j.ijhydene.2023.07.033

[48] Cannio M, et al. Smart catalyst deposition by 3D printing for polymer electrolyte membrane fuel cell manufacturing. Renew Energy Jan. 2021;163:414–22. https://doi.org/10.1016/j.renene.2020.08.064.
[49] Shukla S, Stanier D, Saha MS, Stumper J, Secanell M. Analysis of inkjet printed PEFC electrodes with varying platinum loading. J Electrochem Soc Apr. 2016;163(7):F677–87. https://doi.org/10.1149/2.1111607JES/XML.
[50] Taylor AD, Kim EY, Humes VP, Kizuka J, Thompson LT. Inkjet printing of carbon supported platinum 3-D catalyst layers for use in fuel cells. J Power Sources Sep. 2007;171(1):101–6. https://doi.org/10.1016/J.JPOWSOUR.2007.01.024.
[51] Willert A, Tabary FZ, Zubkova T, Santangelo PE, Romagnoli M, Baumann RR. Multilayer additive manufacturing of catalyst-coated membranes for polymer electrolyte membrane fuel cells by inkjet printing. Int J Hydrogen Energy Jun. 2022;47(48):20973–86. https://doi.org/10.1016/J.IJHYDENE.2022.04.197.
[52] Dang QK, Chang PL, Dang TN, Weng F, Uan JY, Wang DA. Ultrasonic spot welds of gas diffusion layer to proton exchange membrane of fuel cells. J Mater Process Technol July 2018;266:208–16. https://doi.org/10.1016/j.jmatprotec.2018.11.004. 2019.
[53] Abderezzak B. Introduction to hydrogen technology. In: Introduction to transfer phenomena in PEM fuel cell. Elsevier; 2018. p. 1–51. https://doi.org/10.1016/B978-1-78548-291-5.50001-9.
[54] Kim H, Lee YJ, Park GG, Park SH, Choi YY, Yoo Y. Fabrication of carbon paper containing PEDOT:PSS for use as a gas diffusion layer in proton exchange membrane fuel cells. Carbon N. Y. Apr. 2015;85:422–8. https://doi.org/10.1016/j.carbon.2014.12.103.
[55] Arisetty S, Prasad AK, Advani SG. Metal foams as flow field and gas diffusion layer in direct methanol fuel cells. J Power Sources Feb. 2007;165(1):49–57. https://doi.org/10.1016/J.JPOWSOUR.2006.12.008.
[56] Zhang F-Y, Advani SG, Prasad AK. Performance of a metallic gas diffusion layer for PEM fuel cells. J Power Sources Jan. 2008;176(1):293–8. https://doi.org/10.1016/j.jpowsour.2007.10.055.
[57] Luo X, et al. Design and fabrication of bipolar plates for PEM water electrolyser. J Mater Sci Technol 2023;146:19–41. https://doi.org/10.1016/j.jmst.2022.10.039.
[58] Porstmann S, Wannemacher T, Drossel WG. A comprehensive comparison of state-of-the-art manufacturing methods for fuel cell bipolar plates including anticipated future industry trends. J Manuf Process Dec. 2020;60:366–83. https://doi.org/10.1016/J.JMAPRO.2020.10.041.
[59] Baroutaji A, et al. Materials in PEM fuel cells. In: Hashmi Saleem, editor. Reference module in materials science and materials engineering. Oxford: Elsevier; 2016. p. 1–11. https://doi.org/10.1016/B978-0-12-803581-8.04006-6 (editor-in-chief).
[60] Wilberforce T, et al. A comprehensive study of the effect of bipolar plate (BP) geometry design on the performance of proton exchange membrane (PEM) fuel cells. Renew Sustain Energy Rev Sep. 2019;111:236–60. https://doi.org/10.1016/J.RSER.2019.04.081.
[61] Atyabi SA, Afshari E. Three-dimensional multiphase model of proton exchange membrane fuel cell with honeycomb flow field at the cathode side. J Clean Prod Mar. 2019;214:738–48. https://doi.org/10.1016/J.JCLEPRO.2018.12.293.
[62] Wilberforce T, et al. Development of Bi-polar plate design of PEM fuel cell using CFD techniques. Int J Hydrogen Energy Oct. 2017;42(40):25663–85. https://doi.org/10.1016/J.IJHYDENE.2017.08.093.
[63] Li X, Sabir I. Review of bipolar plates in PEM fuel cells: flow-field designs. Int J Hydrogen Energy Mar. 2005;30(4):359–71. https://doi.org/10.1016/j.ijhydene.2004.09.019.
[64] Antunes RA, Oliveira MCL, Ett G, Ett V. Corrosion of metal bipolar plates for PEM fuel cells: a review. Int J Hydrogen Energy Apr. 2010;35(8):3632–47. https://doi.org/10.1016/j.ijhydene.2010.01.059.
[65] Hermann A, Chaudhuri T, Spagnol P. Bipolar plates for PEM fuel cells: a review. Int J Hydrogen Energy Sep. 2005;30(12):1297–302. https://doi.org/10.1016/J.IJHYDENE.2005.04.016.
[66] Sánchez-Molina M, Amores E, Rojas N, Kunowsky M. Additive manufacturing of bipolar plates for hydrogen production in proton exchange membrane water electrolysis cells. Int J Hydrogen Energy Nov. 2021;46(79):38983–91. https://doi.org/10.1016/J.IJHYDENE.2021.09.152.
[67] Madheswaran DK, Jayakumar A, Velu R, Raj R, Varuvel EG. Polymer based flow field plates for polymer electrolyte membrane fuel cell and the scope of additive manufacturing: a techno-economic review. Int J Energy Res Nov. 2022;46(14):19737–61. https://doi.org/10.1002/ER.8645.
[68] IRENA, "Green hydrogen cost reduction." Accessed: Aug. 29, 2022. [Online]. Available: https://www.irena.org//publications/2020/Dec/Green-hydrogen-cost-reduction.
[69] Zhang C, Ma J, Liang X, Luo F, Cheng R, Gong F. Fabrication of metallic bipolar plate for proton exchange membrane fuel cells by using polymer powder medium based flexible forming. J Mater Process Technol 2018;262(February):32–40. https://doi.org/10.1016/j.jmatprotec.2018.06.014.
[70] Lee HS, Kim HJ, Kim SG, Ahn SH. Evaluation of graphite composite bipolar plate for PEM (proton exchange membrane) fuel cell: electrical, mechanical, and molding properties. J Mater Process Technol 2007;187–188:425–8. https://doi.org/10.1016/j.jmatprotec.2006.11.213.
[71] Kargar-Pishbijari H, Hosseinipour SJ, Jamshidi Aval H. A novel method for manufacturing microchannels of metallic bipolar plate fuel cell by the hot metal gas forming process. J Manuf Process 2020;55(January 2019):268–75. https://doi.org/10.1016/j.jmapro.2020.04.040.
[72] Huang P, et al. Stainless steel bipolar plate fuel cell with different flow field structures prepared by laser additive manufacturing. Int J Heat Mass Tran Feb. 2022;183:122186. https://doi.org/10.1016/J.IJHEATMASSTRANSFER.2021.122186.
[73] Scotti G, et al. Laser additive manufacturing of stainless steel micro fuel cells. J Power Sources Dec. 2014;272:356–61. https://doi.org/10.1016/j.jpowsour.2014.08.096.
[74] Shrinivas Mahale R, et al. Processes and applications of metal additive manufacturing. Mater Today Proc Jan. 2022;54:228–33. https://doi.org/10.1016/j.matpr.2021.08.298.
[75] ISO/ASTM. ISO/ASTM 52900:2015, standard terminology for additive manufacturing– general principles-terminology. 2015. Accessed: Aug. 27, 2022. [Online]. Available: https://www.iso.org/standard/69669.html#:~:text=Abstract,intospecificfieldsofapplication.
[76] Tofail SAM, Koumoulos EP, Bandyopadhyay A, Bose S, O'Donoghue L, Charitidis C. Additive manufacturing: scientific and technological challenges, market uptake and opportunities. Mater Today Jan. 2018;21(1):22–37. https://doi.org/10.1016/J.MATTOD.2017.07.001.
[77] Baroutaji A, Arjunan A, Stanford M, Robinson J, Olabi AG. Deformation and energy absorption of additively manufactured functionally graded thickness thin-walled circular tubes under lateral crushing. Eng Struct Jan.

Please cite this article as: Baroutaji A et al., Additive manufacturing for Proton Exchange Membrane (PEM) hydrogen technologies: merits, challenges, and prospects, International Journal of Hydrogen Energy, https://doi.org/10.1016/j.ijhydene.2023.07.033

2021;226:111324. https://doi.org/10.1016/J.ENGSTRUCT.2020.111324.
[78] Robinson J, Arjunan A, Baroutaji A, Stanford M. Mechanical and thermal performance of additively manufactured copper, silver, and copper-silver alloys. Proc Inst Mech Eng Part L J Mater Des Appl 2021. https://doi.org/10.1177/14644207211040929.
[79] Arjunan A, Demetriou M, Baroutaji A, Wang C. Mechanical performance of highly permeable laser melted Ti6Al4V bone scaffolds. J Mech Behav Biomed Mater 2020. https://doi.org/10.1016/j.jmbbm.2019.103517.
[80] Baroutaji A, Arjunan A, Robinsion J, Ramadan M, Abdelkareem MA, Olabi A-G. Metallic meta-biomaterial as biomedical implants. Encycl. Smart Mater Jan. 2022:70–80. https://doi.org/10.1016/B978-0-12-815732-9.00117-0.
[81] What is directed energy deposition (DED)? - twi." 2022 https://www.twi-global.com/technical-knowledge/faqs/directed-energy-deposition (accessed Jul. 30, 2022).
[82] Hemmasian Ettefagh A, Guo S, Raush J. Corrosion performance of additively manufactured stainless steel parts: a review. In: Additive manufacturing, vol. 37. Elsevier B.V.; Jan. 01, 2021. https://doi.org/10.1016/j.addma.2020.101689.
[83] Towne S, Viswanathan V, Holbery J, Rieke P. Fabrication of polymer electrolyte membrane fuel cell MEAs utilizing inkjet print technology. J Power Sources Sep. 2007;171(2):575–84. https://doi.org/10.1016/j.jpowsour.2007.07.017.
[84] Wang Z, Nagao Y. Effects of Nafion impregnation using inkjet printing for membrane electrode assemblies in polymer electrolyte membrane fuel cells. Electrochim Acta May 2014;129:343–7. https://doi.org/10.1016/j.electacta.2014.02.133.
[85] Cano-Vicent A, et al. Fused deposition modelling: current status, methodology, applications and future prospects. In: Additive manufacturing, vol. 47. Elsevier B.V.; Nov. 01, 2021. https://doi.org/10.1016/j.addma.2021.102378.
[86] Mo J, Dehoff RR, Peter WH, Toops TJ, Green JB, Zhang FY. Additive manufacturing of liquid/gas diffusion layers for low-cost and high-efficiency hydrogen production. Int J Hydrogen Energy Jan. 2016;41(4):3128–35. https://doi.org/10.1016/J.IJHYDENE.2015.12.111.
[87] Agudelo MCB, Hampe M, Reiber T, Abele E. Investigation of porous metal-based 3D-printed anode GDLs for tubular high temperature proton exchange membrane fuel cells. Mater May 2020;13(9):2096. https://doi.org/10.3390/MA13092096. 2020, Vol. 13, Page 2096.
[88] Jayakumar A, Ramos M, Al-Jumaily A. A novel 3D printing technique to synthesise gas diffusion layer for PEM fuel cell application. ASME Int. Mech. Eng. Congr. Expo. Proc. Feb. 2017;6B. https://doi.org/10.1115/IMECE2016-65554. 2016.
[89] Bourell DL, Leu MC, Chakravarthy K, Guo N, Alayavalli K. Graphite-based indirect laser sintered fuel cell bipolar plates containing carbon fiber additions. CIRP Ann - Manuf Technol 2011;60(1):275–8. https://doi.org/10.1016/j.cirp.2011.03.105.
[90] Chen S, Bourell DL, Wood KL. Fabrication of PEM fuel cell bipolar plates by indirect SLS. Proc. SFF Symposium 2004:244–56.
[91] Hudkins JR, Wheeler DG, Peñ B, Berlinguette CP. Rapid prototyping of electrolyzer flow field plates. Energy Environ Sci 2016;9:3417. https://doi.org/10.1039/c6ee01997h.
[92] Chisholm G, Kitson PJ, Kirkaldy ND, Bloor LG, Cronin L. 3D printed flow plates for the electrolysis of water: an economic and adaptable approach to device manufacture. Energy Environ Sci Aug. 2014;7(9):3026–32. https://doi.org/10.1039/C4EE01426J.
[93] Dawson RJ, Patel AJ, Rennie AEW, White S. An investigation into the use of additive manufacture for the production of metallic bipolar plates for polymer electrolyte fuel cell stacks. J Appl Electrochem Apr. 2015;45(7):637–45. https://doi.org/10.1007/S10800-015-0832-1. 2015 457.
[94] Yang G, et al. Additive manufactured bipolar plate for high-efficiency hydrogen production in proton exchange membrane electrolyzer cells. Int J Hydrogen Energy May 2017;42(21):14734–40. https://doi.org/10.1016/J.IJHYDENE.2017.04.100.
[95] Lyons KS, Gould BD. Lightweight titanium metal bipolar plates for PEM fuel cells. Mater Sci Forum 2017;879:613–8. https://doi.org/10.4028/WWW.SCIENTIFIC.NET/MSF.879.613.
[96] Zhang J, Huang P, Ding H, Xin D, Sun S. Investigation of the three-dimensional flow field for proton exchange membrane fuel cell with additive manufactured stainless steel bipolar plates: numerical simulation and experiments. Energy Apr. 2023;269:126709. https://doi.org/10.1016/j.energy.2023.126709. Accessed: May 16, 2023. [Online]. Available:.
[97] Scotti G, Kanninen P, Matilainen VP, Salminen A, Kallio T. Stainless steel micro fuel cells with enclosed channels by laser additive manufacturing. Energy Jul. 2016;106:475–81. https://doi.org/10.1016/j.energy.2016.03.086.
[98] Trogadas P, et al. A lung-inspired approach to scalable and robust fuel cell design. This J. is Cite this Energy Environ. Sci 2018;11(1):136. https://doi.org/10.1039/c7ee02161e.
[99] Yang G, et al. Bipolar plate development with additive manufacturing and protective coating for durable and high-efficiency hydrogen production. J Power Sources Aug. 2018;396:590–8. https://doi.org/10.1016/J.JPOWSOUR.2018.06.078.
[100] Gould BD, et al. Performance and limitations of 3D-printed bipolar plates in fuel cells. ECS J. Solid State Sci. Technol. Feb. 2015;4(4):P3063–8. https://doi.org/10.1149/2.0091504JSS/XML.
[101] Yang G, et al. Fully printed and integrated electrolyzer cells with additive manufacturing for high-efficiency water splitting. Appl Energy Apr. 2018;215:202–10. https://doi.org/10.1016/J.APENERGY.2018.02.001.
[102] Litster S, McLean G. PEM fuel cell electrodes. J Power Sources May 03, 2004;130(1–2):61–76. https://doi.org/10.1016/j.jpowsour.2003.12.055.
[103] Breitwieser M, et al. Simple fabrication of 12 μm thin nanocomposite fuel cell membranes by direct electrospinning and printing. J Power Sources Jan. 2017;337:137–44. https://doi.org/10.1016/j.jpowsour.2016.10.094.
[104] Breitwieser M, Klingele M, Britton B, Holdcroft S, Zengerle R, Thiele S. Improved Pt-utilization efficiency of low Pt-loading PEM fuel cell electrodes using direct membrane deposition. Electrochem Commun Nov. 2015;60:168–71. https://doi.org/10.1016/j.elecom.2015.09.006.
[105] Klingele M, Breitwieser M, Zengerle R, Thiele S. Direct deposition of proton exchange membranes enabling high performance hydrogen fuel cells. J Mater Chem 2015;3(21):11239–45. https://doi.org/10.1039/C5TA01341K.
[106] Shukla S, Domican K, Karan K, Bhattacharjee S, Secanell M. Analysis of low platinum loading thin polymer electrolyte fuel cell electrodes prepared by inkjet printing. Electrochim Acta Feb. 2014;156:289–300. https://doi.org/10.1016/j.electacta.2015.01.028.
[107] Bezerra CAG, Deiner LJ, Tremiliosi-Filho G. Inkjet printed double-layered cathodes for PEM fuel cells. J Electrochem

Please cite this article as: Baroutaji A et al., Additive manufacturing for Proton Exchange Membrane (PEM) hydrogen technologies: merits, challenges, and prospects, International Journal of Hydrogen Energy, https://doi.org/10.1016/j.ijhydene.2023.07.033

Soc Aug. 2020;167(12):124503. https://doi.org/10.1149/1945-7111/ABA6CA.
[108] Bürger I, Sourmelis Terzopoulos VE, Kretschmer C, Kölbig M, Brack C, Linder M. Lightweight reactor design by additive manufacturing for preheating applications using metal hydrides. Int J Hydrogen Energy Aug. 2021;46(56):28686–99. https://doi.org/10.1016/J.IJHYDENE.2021.06.091.
[109] Lei HY, et al. Feasibility of preparing additive manufactured porous stainless steel felts with mathematical micro pore structure as novel catalyst support for hydrogen production via methanol steam reforming. Int J Hydrogen Energy Sep. 2019;44(45):24782–91. https://doi.org/10.1016/j.ijhydene.2019.07.187.
[110] Kreider MC, et al. Toward 3D printed hydrogen storage materials made with ABS-MOF composites. Polym Adv Technol Feb. 2018;29(2):867–73. https://doi.org/10.1002/PAT.4197.
[111] Baroutaji A, Carton JG, Oladoye AM, Stokes J, Twomey B, Olabi AG. Ex-situ evaluation of PTFE coated metals in a proton exchange membrane fuel cell environment. Surf Coating Technol 2016;323:10–7. https://doi.org/10.1016/j.surfcoat.2016.11.105.
[112] Örnek C, Idris SAM, Reccagni P, Engelberg DL. Atmospheric-induced stress corrosion cracking of grade 2205 duplex stainless steel—effects of 475 °C embrittlement and process orientation. Met Jul. 2016;6(7):167. https://doi.org/10.3390/MET6070167. 2016, Vol. 6, Page 167.
[113] Örnek C, Engelberg DL. Towards understanding the effect of deformation mode on stress corrosion cracking susceptibility of grade 2205 duplex stainless steel. Mater Sci Eng, A Jun. 2016;666:269–79. https://doi.org/10.1016/j.msea.2016.04.062.
[114] De Bruycker E, et al. Corrosion testing of a heat treated 316 L functional Part Produced by selective laser melting. Mater Sci Appl Mar. 2017;8(3):223–33. https://doi.org/10.4236/MSA.2017.83015.
[115] Tawfik H, Hung Y, Mahajan D. Metal bipolar plates for PEM fuel cell—a review. J Power Sources Jan. 2007;163(2):755–67. https://doi.org/10.1016/j.jpowsour.2006.09.088.
[116] Kong D, et al. Heat treatment effect on the microstructure and corrosion behavior of 316L stainless steel fabricated by selective laser melting for proton exchange membrane fuel cells. Electrochim Acta Jun. 2018;276:293–303. https://doi.org/10.1016/j.electacta.2018.04.188.
[117] Vukkum VB, Gupta RK. Review on corrosion performance of laser powder-bed fusion printed 316L stainless steel: effect of processing parameters, manufacturing defects, post-processing, feedstock, and microstructure. Mater. Des.; Jul. 2022. p. 110874. https://doi.org/10.1016/J.MATDES.2022.110874.
[118] Sander G, et al. Corrosion of additively manufactured alloys: a review. Corrosion Dec. 2018;74(12):1318–50. https://doi.org/10.5006/2926.
[119] Lodhi MJK, Deen KM, Haider W. Corrosion behavior of additively manufactured 316L stainless steel in acidic media. Materialia Oct. 2018;2:111–21. https://doi.org/10.1016/j.mtla.2018.06.015.
[120] Miller JT, Martin HJ, Cudjoe E. Comparison of the effects of a sulfuric acid environment on traditionally manufactured and additive manufactured stainless steel 316L alloy. Addit Manuf Oct. 2018;23:272–86. https://doi.org/10.1016/j.addma.2018.08.023.
[121] Geenen K, Röttger A, Theisen W. Corrosion behavior of 316L austenitic steel processed by selective laser melting, hot-isostatic pressing, and casting. Mater Corros Jul. 2017;68(7):764–75. https://doi.org/10.1002/MACO.201609210.
[122] Kong D, et al. Superior resistance to hydrogen damage for selective laser melted 316L stainless steel in a proton exchange membrane fuel cell environment. Corrosion Sci Apr. 2020;166. https://doi.org/10.1016/j.corsci.2019.108425.
[123] Svendby J, Bjelland Ø, Bokach D, Solheim BGB. The use of additive manufactured Inconel 625 as Bipolar Plate for the high temperature proton electrolyte membrane fuel cell. Procedia Struct Integr Jan. 2021;34:51–8. https://doi.org/10.1016/J.PROSTR.2021.12.008.
[124] Cheng H, et al. Tuning the microstructure to improve corrosion resistance of additive manufacturing high-entropy alloy in proton exchange membrane fuel cells environment. Corrosion Sci Apr. 2023;213:110969. https://doi.org/10.1016/j.corsci.2023.110969. Accessed: May 08, 2023. [Online]. Available:.
[125] Bertsch KM, Nagao A, Rankouhi B, Kuehl B, Thoma DJ. Hydrogen embrittlement of additively manufactured austenitic stainless steel 316 L. Corrosion Sci Nov. 2021;192. https://doi.org/10.1016/j.corsci.2021.109790.
[126] Papavinasam S. Mechanisms. Corros. Control Oil Gas Ind Jan. 2014:249–300. https://doi.org/10.1016/B978-0-12-397022-0.00005-4.
[127] Baek SW, Song EJ, Kim JH, Jung M, Baek UB, Nahm SH. Hydrogen embrittlement of 3-D printing manufactured austenitic stainless steel part for hydrogen service. Scripta Mater Mar. 2017;130:87–90. https://doi.org/10.1016/j.scriptamat.2016.11.020.
[128] Lee DH, Sun B, Lee S, Ponge D, Jägle EA, Raabe D. Comparative study of hydrogen embrittlement resistance between additively and conventionally manufactured 304L austenitic stainless steels. Mater Sci Eng, A Jan. 2021;803. https://doi.org/10.1016/j.msea.2020.140499.
[129] Silverstein R, Eliezer D. Hydrogen trapping in 3D-printed (additive manufactured) Ti-6Al-4V. Mater Char Oct. 2018;144:297–304. https://doi.org/10.1016/j.matchar.2018.07.029.
[130] Wang Y, Ruiz Diaz DF, Chen KS, Wang Z, Adroher XC. Materials, technological status, and fundamentals of PEM fuel cells – a review. In: Materials today, vol. 32. Elsevier B.V.; Jan. 01, 2020. p. 178–203. https://doi.org/10.1016/j.mattod.2019.06.005.
[131] Tarancón A, et al. 2022 roadmap on 3D printing for energy. JPhys Energy Jan. 2022;4(1). https://doi.org/10.1088/2515-7655/ac483d.
[132] Arjunan A, Robinson J, Al Ani E, Heaselgrave W, Baroutaji A, Wang C. Mechanical performance of additively manufactured pure silver antibacterial bone scaffolds. J Mech Behav Biomed Mater Dec. 2020;112:104090. https://doi.org/10.1016/j.jmbbm.2020.104090.
[133] Chen S, Tong Y, Liaw PK. Additive manufacturing of high-entropy alloys: a review. Entropy 2018. https://doi.org/10.3390/e20120937.
[134] Shahi RR, Gupta AK, Kumari P. Perspectives of high entropy alloys as hydrogen storage materials. Int J Hydrogen Energy 2022. https://doi.org/10.1016/j.ijhydene.2022.02.113.
[135] Zhang Y, Wang D, Wang S. High-entropy alloys for electrocatalysis: design, characterization, and applications. Small Feb. 2022;18(7):2104339. https://doi.org/10.1002/SMLL.202104339.
[136] Qiu HJ, et al. Nanoporous high-entropy alloys for highly stable and efficient catalysts. J Mater Chem Mar. 2019;7(11):6499–506. https://doi.org/10.1039/C9TA00505F.

Please cite this article as: Baroutaji A et al., Additive manufacturing for Proton Exchange Membrane (PEM) hydrogen technologies: merits, challenges, and prospects, International Journal of Hydrogen Energy, https://doi.org/10.1016/j.ijhydene.2023.07.033